https://doi.org/10.5194/acp-2023-8
Preprint. Discussion started: 16 January 2023
© Author(s) 2023. CC BY 4.0 License.

Atmospheric Chemistry and Physics Discussions

The Important Contribution of Secondary Formation and Biomass Burning to Oxidized Organic Nitrogen (OON) in a Polluted Urban Area: Insights from In Situ FIGAERO-CIMS Measurements

Yiyu Cai[1,2,3,4,5&], Chenshuo Ye[6&], Wei Chen[1,2,3,4,5], Weiwei Hu[1,2,3,4], Wei Song[1,2,3,4], Yuwen Peng[7,8], Shan Huang[7,8], Jipeng Qi[7,8], Sihang Wang[7,8], Chaomin Wang[7,8], Caihong Wu[7,8], Zelong Wang[7,8], Baolin Wang[9], Xiaofeng Huang[10], Lingyan He[10], Sasho Gligorovski[1,2,3,4], Bin Yuan[7,8], Min Shao[7,8], Xinming Wang[1,2,3,4]

[1]State Key Laboratory of Organic Geochemistry, Guangzhou Institute of Geochemistry, Chinese Academy of Sciences, Guangzhou 510640. China
[2]CAS Center for Excellence in Deep Earth Science, Guangzhou, 510640, China
[3]Guangdong-Hong Kong-Macao, Joint Laboratory for Environmental Pollution and Control, Guangzhou Institute of Geochemistry, Chinese Academy of Science, Guangzhou 510640, China
[4]Guangdong Provincial Key Laboratory of Environmental Protection and Resources Utilization, Chinese Academy of Science, Guangzhou 510640, China
[5]University of Chinese Academy of Sciences, Beijing 100049, China
[6]Guangdong Provincial Academy of Environmental Science, Guangzhou, 510640, China
[7]Institute for Environmental and Climate Research, Jinan University, Guangzhou 511443, China
[8]Guangdong-Hongkong-Macau Joint Laboratory of Collaborative Innovation for Environmental Quality, Guangzhou 511443, China
[9]School of Environmental Science and Engineering, Qilu University of Technology, Jinan 250353, China
[10]Key Laboratory for Urban Habitat Environmental Science and Technology, School of Environment and Energy, Peking University Shenzhen Graduate School, Shenzhen, 518055, China
&Yiyu Cai and Chenshuo Ye contributed equally to this work.

Correspondence to: Weiwei Hu (weiweihu@gig.ac.cn); Bin Yuan (byuan@jnu.edu.cn).

Abstract. To investigate the sources and formation mechanism of oxidized organic nitrogen (OON), field measurements of OON were conducted using an iodide-adduct chemical ionization mass spectrometer equipped with a Filter Inlet for Gases and AEROsols (FIGAERO-CIMS) during fall of 2018 in the megacity of Guangzhou, China. Using levoglucosan as tracer of biomass burning emissions, the results show that biomass burning (49%) and secondary formation (51%) accounted for comparable fractions to the total particle-phase OON (pOON), while 24% and 76% to the gas-phase OON (gOON), respectively, signifying the important contribution of biomass burning to pOON and secondary formation to gOON in this urban area. Calculations of production rates of gas-phase organic nitrates (gON) indicated that hydroxyl radical (42%) and nitrate radical (NO_3) (49%) oxidation pathways potentially dominated the secondary formation of gON. High concentration of NO_3 radical during the afternoon daytime was observed, demonstrating that the daytime NO_3 oxidation might be more important than the previous recognition. Monoterpenes, found to be major precursor of secondary gON, were mainly from anthropogenic emissions in this urban area. The ratio of secondary pOON to O_x ($[O_x] = [O_3] + [NO_2]$) increased as a function of relative humidity and aerosol surface area, indicating that heterogeneous reaction might be an important formation pathway for secondary pOON. Finally, the highly oxidized gOON and pOON with 6 to 11 oxygen atoms were observed, highlighting the complex secondary reaction processes of OON in the ambient air. Overall, our results can improve the understanding of the sources and dynamic variation of OON in urban atmosphere.

https://doi.org/10.5194/acp-2023-8
Preprint. Discussion started: 16 January 2023
© Author(s) 2023. CC BY 4.0 License.

Atmospheric Chemistry and Physics Discussions

1 Introduction

Oxidized organic nitrogen (OON, including organic nitrates (ONs) and nitroaromatics) , acting as an important reservoir of atmospheric nitrogen oxides (NO_x = NO + NO_2) (Fisher et al., 2016; Romer Present et al., 2020; Romer et al., 2016; Ditto et al., 2022), substantially influence the NO_x cycling, formation of ozone (O_3) (Farmer et al., 2011; Perring et al., 2013), and secondary organic aerosol (SOA) (Lee et al., 2016; Rollins et al., 2012), thus affect air quality, climate, and ecosystem nutrient cycling (Kiendler-Scharr et al., 2016; Pye et al., 2015). A comprehensive and in-depth understanding of dynamic variations of *in situ* OON (including in gas phase (gOON) and particle phase (pOON)) and their sources is crucial for accurately assessing their environmental impacts.

With the rapid development of measurement techniques, high-time resolution measurement of OONs has become more available. Currently, online measurement of OONs can be conducted by the following routes: (I) by thermodenuder dissociation to NO_2 and then detection by laser-induced fluorescence (TD-LIF) (Day et al., 2002; Rollins et al., 2010) or cavity-related spectroscopy (Keehan et al., 2020; Sadanaga et al., 2016); (II) by using aerosol mass spectrometer (AMS) (Decarlo et al., 2006) based on NO_2^+/NO^+ apportionment (Farmer et al., 2010; Fry et al., 2013; Hao et al., 2014; Day et al., 2022) and/or thermodenuder (Xu et al., 2021); and (III) by using chemical ionization mass spectrometer (CIMS) with different ionization sources, typically with iodide-adduct chemistry (Huang et al., 2019; Lee et al., 2014; Lee et al., 2016) or extractive electrospray ionization (Bell et al., 2021; Lopez-Hilfiker et al., 2019; Pospisilova et al., 2020). Although the first two methods can quantify nitrate functional group (–ONO_2 or -NO_2) in bulk; CIMS, by taking advantage of soft ionization, can provide information on molecular compositions and better comprehend particle-phase ONs (pON) and nitroaromatics at the molecular level (Lee et al., 2014; Pospisilova et al., 2020; Wang et al., 2020b; Salvador et al., 2021). In general, nitro-aromatics have also been included in the quantification of ONs by CIMS under negative ionization mode, due to the difficulty encountered in distinguishing the nitro functional group (–NO_2) from –ONO_2 and –NO_2 groups based solely on chemical formulas of ions (Huang et al., 2019).So far, gOON and pOON (containing 4–12 oxygen atoms) formed from multiple oxidation process of volatile organic compounds (VOCs) have been quantified by a high-resolution time-of-flight CIMS installed with a Filter Inlet for Gases and AEROsols (FIGAERO-CIMS) in the forests (Lee et al., 2018; Lee et al., 2016) and at a rural site (Huang et al., 2019). However, limited measurement results were reported in the polluted urban areas (Le Breton et al., 2019).

Both primary emission and secondary formation can contribute to mass concentrations of ambient OON. Biomass burning and/or fossil fuel combustion have been suggested to be important primary emission sources of gOON (Liu et al., 2017; Palm et al., 2020; Peng et al., 2021) and pOON (Gaston et al., 2016; Mohr et al., 2013; Wang et al., 2019; Zhang et al., 2016). Furthermore, secondary formation of OON in biomass burning plumes has also been observed. For example, Juncosa Calahorrano et al. (2021)

https://doi.org/10.5194/acp-2023-8
Preprint. Discussion started: 16 January 2023
© Author(s) 2023. CC BY 4.0 License.

Atmospheric Chemistry and Physics Discussions

observed the existence of gOON in aged plumes of wildfires. Kodros et al. (2020) showed that pOON could not only be directly emitted from laboratory-generated biomass burning emissions but also formed quickly through nitrate radical (NO_3) oxidation within biomass burning plumes. Based on aircraft measurements, Palm et al. (2020) found that the VOCs and vapors evaporated from primary biomass burning could be quickly subjected to radical-driven oxidation, thus contributing to the formation of SOA including nitro-aromatics. For the secondary formation pathway in ambient air, gOON is formed mainly through the oxidation of VOCs by hydroxyl radical (OH), NO_3, and ozone in the presence of NO_x (Ng et al., 2017; Perring et al., 2013). Functionalization of gOON in ambient air reduces their volatility, leading to condensation of gOON on particles to form secondary pOON (Capouet and Müller, 2006).

Previous studies indicated that the oxidation of biogenic VOCs by NO_3 dominated gOON formation at a forest-urban site in Germany (56% of average gOON production rate) (Sobanski et al., 2017), as well as at a boreal forest site in the Finland (70% of total gOON production rate) (Liebmann et al., 2019) and the southeast US (84% of monoterpene organic nitrate mass) (Ayres et al., 2015; Pye et al., 2015). For urban areas, the contributions of the above-mentioned three secondary formation pathways to total gOON remain poorly understood (Yu et al., 2019). Initiation of oxidation by OH under high NO_x condition is traditionally regarded as the main formation pathway for urban OONs during the day (Perring et al., 2013). However, Hamilton et al. (2021) recently found that a large fraction of isoprene-derived OONs was formed through unexpected NO_3 oxidation pathway in the afternoon in Beijing urban area. Thus, a better understanding of the OON sources and formation mechanism in urban areas is still needed.

In this study, quantitative measurements of gOON and pOON were carried out using a high-resolution time-of-flight FIGAERO-CIMS and an AMS in a Chinese megacity. The contributions of biomass burning and secondary formation to ambient total gOON and pOON were quantified, and the secondary oxidation pathways were systematically explored based on the production rates of gON. Finally, the molecular compositions of ambient OON were comprehensively investigated.

2 Experimental Methods

2.1 Sampling site.

Measurements were conducted on the campus of Guangzhou Institute of Geochemistry, Chinese Academy of Sciences (23.14°N, 113.36°E) in the urban area of megacity Guangzhou, during the coordinated campaign "Particles, Radicals, and Intermediates from oxidation of primary Emissions over the Great Bay Area" (PRIDE-GBA) (Wu et al., 2020). The observation site is located 25 m above the ground on the ninth floor of the highest building on the campus. The campus was surrounded with industrialized and urbanized downtown areas under a typically subtropical climate, thus strongly influenced by both anthropogenic and biogenic emissions, as shown in Fig. S1. The average ambient temperature and relative humidity (RH) during the campaign

https://doi.org/10.5194/acp-2023-8
Preprint. Discussion started: 16 January 2023
© Author(s) 2023. CC BY 4.0 License.

Atmospheric Chemistry and Physics Discussions

were 23.7 ± 2.9°C and 71.9 ± 17.4%, respectively. The site was mostly affected by northerly winds with an average speed of 4.5 ± 2.18 m s^{-1}.

2.2 Measurement and analysis.

2.2.1 Operation of FIGAERO-CIMS

During the campaign, a CIMS installed with a long time-of-flight detector (10000 < m/Δm < 11000) with an iodide source (Aerodyne Research Inc, USA) was deployed (Lee et al., 2014; Wang et al., 2020d). The FIGAERO inlet was installed with the CIMS to measure speciated gOON and pOON (Lopez-Hilfiker et al., 2014; Bannan et al., 2019; Schobesberger et al., 2018; Thornton et al., 2020). The detailed performance and calibration information of the CIMS can be found in a recent paper about this campaign (Ye et al., 2021). A brief description is introduced here. A $PM_{2.5}$ cyclone inlet and a Nafion dryer (Perma Pure, model PD-07018T-12MSS) were set ahead of the particle sampling inlet of the FIGAERO. To measure the gOON and pOON, the FIGEARO was operated alternately at two main stages during the measurement: (i) For the first 24 min in one hour cycle, ambient air was continuously sampled into two inlets, i.e., gas and particle inlets. The gas inlet was connected to an ion-molecule reaction region (IMR) of the CIMS. An X-ray source was used in this campaign, which has lower ionization efficiency compared to the polonium-210 radioactive source used in the previous studies (Faxon et al., 2018; Lee et al., 2021; Palm et al., 2019). Therefore, a high pressure (370–390 mbar) in the IMR than previous studies (e.g., 93–200 mbar) (Faxon et al., 2018; Lee et al., 2021; Palm et al., 2019) was used to achieve similar strength of reagent ions in the CIMS system. The sampled VOCs were first ionized in the IMR ($VOC{\bullet}I^-$), in which the primary ions were generated by flowing 2 mL/min 1000 ppm methyl iodide in 2.4 L/min N_2 through the X-ray source, and then moved into the mass spectrometer for measurement at a resolution of 1 s. Moreover, the ambient air was also introduced in the particle sampling inlet where a sliding Teflon tray held a polytetrafluoroethylene (PTFE) membrane filter (Zefluor®, Pall Inc., USA) for aerosol collection for 24 min. (ii) Next, after 24 min when the gas-phase measurement was completed, a linear actuator was used to move the Teflon tray on which the filter was placed in front of the IMR, while the gas phase inlet was blocked. Then, ultrahigh-purity N_2 gas at a flow rate of 2 L min^{-1} was passed through a stainless steel "heating tube" to thermally desorb the collected particles on the filter into gas phase, and then into the IMR and mass spectrometer for measurement. The temperature of N_2 flow was ramped from room temperature to 175 °C in 12 min and then kept at 175 °C for another 20 min.

The background signal of the gas-phase measurement was determined by pure N_2 signal at the last 3 min within the 24-min sampling time (Palm et al., 2019). The background signal of the particle measurement was determined by the measured signals from every sixth 1-h running cycle, in which particle-free air was obtained with ambient air passing through a High-Efficiency Particulate Air (HEPA) filter set ahead of the FIGAERO filter (Ye et al., 2021). The TofWare software (version 3.0.3) was used to perform high-resolution peak fitting of the CIMS mass spectra.

https://doi.org/10.5194/acp-2023-8
Preprint. Discussion started: 16 January 2023
© Author(s) 2023. CC BY 4.0 License.

Atmospheric Chemistry and Physics Discussions

2.2.2 Oxidized Organic nitrogen quantification based on CIMS measurement

Based on the CIMS measurement, speciated OON (nitrogen-containing oxygenated hydrocarbons, 339 closed-shell compounds with oxygen versus carbon atom ratio no less than 3, $C_{\geq 1}H_{\geq 1}O_{\geq 3}N_{1-2}$) both gas and particle phases were quantified. In this study, nitro-aromatics were also a subset of OON due to (I) their similar chemical and optical properties as the bulk OON compounds (He et al., 2021; Lin et al., 2017) and (II) interferences between ONs and nitro-aromatics in the CIMS measurement due to desorption and fragmentation (Ye et al., 2021). The composition of OON was mainly contributed by the CHON (one nitrogen atom containing species), and the $CHON_2$ (two nitrogen atom containing species) only contributed 6.8% of the gOON and 8.3% of the pOON.

For quantification, 39 species in total including levoglucosan ($C_6H_{10}O_5$), 4-nitrophenol ($C_6H_5NO_3$), 2,4-dinitrophenol ($C_6H_4N_2O_5$), and 4-nitrocatechol ($C_6H_4NO_4$) were calibrated with standard compounds, where the effect of humidity on the sensitivities was also accounted for (Ye et al., 2021). For other uncalibrated species, a voltage scanning procedure was carried out every few days throughout the campaign to determine their sensitivities (including ON species) (Lee et al., 2016; Lopez-Hilfiker et al., 2016). Relative transmission efficiency as a Gaussian curve of m/z was also fitted and considered for the final ON quantification.

In summary, nitro-aromatics, i.e., nitrophenol ($C_6H_5NO_3$), methyl nitrophenol ($C_7H_7NO_3$), dinitrophenol ($C_6H_4N_2O_5$), nitrocatechol ($C_6H_5NO_4$), methyl nitrocatechol ($C_7H_7NO_4$), and nitrosalicylic acid ($C_7H_5NO_5$), which were assumed to be identified with the ions containing the same molecule compositions detected by the CIMS (Wang et al., 2018; Wang and Li, 2021; Chen et al., 2021b), accounted for 18% and 5% of total gOON and pOON mass concentrations, respectively. Thus, ONs were the dominated components in OON compound observed in this campaign. Note that there might also be other nitrogen-containing species rather than nitro-aromatics that contributed to these ions. For the total OON, the Iodide-CIMS may underestimate or poorly detect some types of OON, e.g., simple alkyl or keto nitrates (Lee et al., 2016). Moreover, the thermal fragmentation reactions that result from heating on the FIGAERO filter may also lead to underestimation of OON due to the loss of the nitrogen-containing groups, such as peroxy nitrates, which have the propensity to thermally dissociate into NO_2 and other non-nitrogen-containing species (Lee et al., 2016).

The levoglucosan ($C_6H_{10}O_5$) in the particle phase measured using the CIMS was used as a tracer for biomass burning emission herein (Bhattarai et al., 2019). The averaged photochemical age was 0.2 days during the night to maximum 0.5 days in the daytime (Chen et al., 2021a), which was lower than the lifetime of levoglucosan (>1 day –26 days) determined in laboratory and field studies (Hennigan et al., 2010; Hoffmann et al., 2010; Lai et al., 2014; Bai et al., 2013; Bhattarai et al., 2019). It suggests the levoglucosan shall be stable for being the tracer of biomass burning emissions.

https://doi.org/10.5194/acp-2023-8
Preprint. Discussion started: 16 January 2023
© Author(s) 2023. CC BY 4.0 License.

Atmospheric Chemistry and Physics Discussions

2.2.3 Other instruments

Besides the CIMS, a high-resolution time-of-flight aerosol mass spectrometer (HR-ToF-AMS, Aerodyne Research Inc., hereinafter referred to as "AMS") was used to provide online quantitative measurement of submicron non-refractory aerosols (PM_1) at a time resolution of 4 min (Canagaratna et al., 2007; Decarlo et al., 2006). In addition to the total organic aerosol (OA), the mass concentration of $–ONO_2$ group from pON ($pOrgNO_{3,AMS}$) was also estimated by NO_2^+/ NO^+ ratio method (Farmer et al., 2010; Fry et al., 2013; Day et al., 2022), positive matrix factorization method (Hao et al., 2014), and thermodenuder method (Xu et al., 2021) based on the AMS data. The comparative analysis among the CIMS and these three methods by the AMS aided in evaluating the measurement accuracy of OON in this study. Detailed description and intercomparison of these three methods can be found in the supporting information (Text S1), where some insights into the pros and cons of the AMS-based methods are also presented. Herein, pON estimated by NO_2^+/ NO^+ ratio method was selected as representative data for the following discussion due to the better performance achieved by this method. More detailed information on calibrations and operations of the AMS during this campaign can be found elsewhere (Chen et al., 2021a).

VOCs were measured by online gas chromatography-mass spectrometry and using a flame ionization detector (GC-MS/FID) (Wuhan Tianhong Instrument Co., Ltd.) at a time resolution of 1 h and by proton transfer reaction time-of-flight mass spectrometry (PTR-ToF-MS, IONICON Analytik) at a time resolution of 10 s (Wu et al., 2020; Yuan et al., 2017). A 56-component VOC gas standard was used for daily calibration of the GC-MS/FID (Wang et al., 2020c). For the PTR-ToF-MS, a 16-component VOC gas standard was used for daily calibration under both dry (RH < 1%) and ambient humidity during the whole campaign, and an additional 23-component VOC gas standard was used during the last period of the campaign (Wang et al., 2020a; Wu et al., 2020). The uncertainties for the VOC measurements by both instruments were below 20%. Trace gases, i.e., O_3 (TL43i), NO/NO_2 (TL42i), and CO (TL48i), were measured using Thermo Fisher Scientific instruments at a time resolution of 1 min (Wang et al., 2020d). Meteorological parameters were measured on a Vantage Pro2 weather station (Davis Instruments) at a time resolution of 10 s.

2.3 Calculation of the production rates of gas-phase oxidized organic nitrogen.

The production rates of gOON from VOCs oxidized by OH, NO_3, and O_3 were calculated using the reactant concentrations and reaction rate coefficients combined with formation branching ratios and yields (Liebmann et al., 2019), of which the detailed calculation process can be found in Text S2. In this calculation, the production rate mainly from organic nitrate were shown. The parameters for secondary nitro-aromatics are not available, thus, was not included here. The concentrations of VOCs and O_3 were obtained from direct measurements, while those of OH was derived from a box model simulation with the Master Chemical Mechanism v3.3.1 (MCM v3.3.1) (Wang et al., 2020c; Wolfe et al., 2016). The NO_3 was calculated based on the measured N_2O_5

https://doi.org/10.5194/acp-2023-8
Preprint. Discussion started: 16 January 2023
© Author(s) 2023. CC BY 4.0 License.

Atmospheric Chemistry and Physics Discussions

by the CIMS (Ye et al., 2021) based on temperature equilibrium between these two species (Brown and Stutz, 2012; Chen et al., 2022). The remaining parameters were obtained from the previous studies (Liebmann et al., 2019; Perring et al., 2013). The different VOC species and corresponding parameters are listed in Table 1. An overall uncertainty of 56% was estimated by the Monte Carlo method through 10,000 calculations in this method. The detailed uncertainties of different parameters can be found in Text S3.

185 **Table 1. The VOC species and their average mass concentrations with standard deviations; The reaction rate coefficients, branch ratios for OH and O_3 pathway and yields for NO_3 pathway used for the calculations of gON production rates.**

OH-initiated pathway VOC species	Average concentration (ppb)	k_{OH} at 298K (cm^3 $molecules^{-1}$ s^{-1})	α^{RO_2}
Isoprene	0.15 ± 0.17	1.00×10^{-10}	0.070
d-Limonene [a]	0.07 ± 0.07	1.70×10^{-10}	0.230
α-pinene [a]	0.07 ± 0.07	5.30×10^{-11}	0.180
Propane	6.23 ± 4.92	1.09×10^{-12}	0.036
iso-Butane	1.56 ± 1.27	2.12×10^{-12}	0.096
n-Butane	2.80 ± 2.35	2.36×10^{-12}	0.077
Cyclopentane	0.09 ± 0.05	4.97×10^{-12}	0.045
iso-Pentane	1.17 ± 1.01	3.60×10^{-12}	0.070
n-Pentane	0.65 ± 0.65	3.80×10^{-11}	0.105
2,2-Dimethylbutane	0.03 ± 0.02	2.23×10^{-12}	0.152
2,3-Dimethylbutane	0.05 ± 0.05	2.23×10^{-12}	0.152
2-Methylpentane	0.26 ± 0.27	5.20×10^{-12}	0.097
3-Methylpentane	0.25 ± 0.25	5.20×10^{-12}	0.109
n-Hexane	0.50 ± 0.75	5.20×10^{-12}	0.141
2,4-Dimethylpentane	0.03 ± 0.03	3.34×10^{-12}	0.140
Methylcyclopentane	0.09 ± 0.09	5.60×10^{-12}	0.140
Cyclohexane	0.05 ± 0.05	6.97×10^{-12}	0.160
n-Heptane	0.09 ± 0.15	6.76×10^{-12}	0.178
Methylcyclohexane	0.07 ± 0.09	9.64×10^{-12}	0.170
n-Octane	0.04 ± 0.05	8.11×10^{-12}	0.226
Nonane	0.03 ± 0.03	9.70×10^{-12}	0.393
n-Decane	0.02 ± 0.02	1.10×10^{-11}	0.417
Benzene	0.43 ± 0.16	1.22×10^{-12}	0.034
Toluene	1.75 ± 1.86	5.96×10^{-12}	0.029
Ethylbenzene	0.28 ± 0.30	7.00×10^{-12}	0.072
m-p-Xylene	0.79 ± 0.82	2.30×10^{-11}	0.074
o-Xylene	0.29 ± 0.31	1.36×10^{-11}	0.081
Isopropylbenzene	0.01 ± 0.01	6.30×10^{-12}	0.110
m-Ethyltoluene	0.03 ± 0.03	1.86×10^{-11}	0.094
p-Ethyltoluene	0.02 ± 0.02	1.18×10^{-11}	0.137
1,3,5-Trimethylbenzene	0.02 ± 0.02	5.76×10^{-11}	0.031
o-Ethyltoluene	0.02 ± 0.02	1.19×10^{-11}	0.106
1,2,4-Trimethylbenzene	0.06 ± 0.06	3.25×10^{-11}	0.105
1,2,3-Trimethylbenzene	0.02 ± 0.01	3.25×10^{-11}	0.119
Propene	0.37 ± 0.37	2.63×10^{-11}	0.015
trans-2-Butene	0.03 ± 0.03	6.40×10^{-11}	0.034
1-Butene	0.07 ± 0.05	3.14×10^{-11}	0.025
cis-2-Butene	0.02 ± 0.02	5.64×10^{-11}	0.034
1-Pentene	0.03 ± 0.02	3.14×10^{-11}	0.059
trans-2-Pentene	0.01 ± 0.02	6.70×10^{-11}	0.064
cis-2-Pentene	0.01 ± 0.01	6.50×10^{-11}	0.064
1-Hexene	0.02 ± 0.01	3.70×10^{-11}	0.055

https://doi.org/10.5194/acp-2023-8
Preprint. Discussion started: 16 January 2023
© Author(s) 2023. CC BY 4.0 License.

Atmospheric Chemistry and Physics Discussions

NO_3-initiated pathway VOC species	Average concentration (ppb)	k_{NO_3} at 298K (cm^3 $molecules^{-1}$ s^{-1})	α_i
Isoprene	0.15 ± 0.17	6.95×10^{-13}	0.700
d-Limonene	0.07 ± 0.07	1.22×10^{-11}	0.670
α-pinene	0.07 ± 0.07	6.21×10^{-12}	0.150
Phenol	0.04 ± 0.03	3.92×10^{-12}	0.251
Cresol	0.03 ± 0.03	1.37×10^{-11}	0.128
Styrene	0.17 ± 0.26	1.50×10^{-12}	0.251 [b]
O_3-initiated pathway VOC species	Average concentration (ppb)	k_{O_3} at 298K (cm^3 $molecules^{-1}$ s^{-1})	α^{O3}
Isoprene	0.15 ± 0.17	1.28×10^{-17}	1.000
d-Limonene	0.07 ± 0.07	2.20×10^{-16}	0.750
α-pinene	0.07 ± 0.07	9.40×10^{-17}	0.800

Note that all the reaction rate coefficients and the formation branching ratios or yields are from MCM v3.3.1 and previous studies (Perring et al., 2013; Liebmann et al., 2019; Atkinson and Arey, 2003). [a] We assumed total monoterpenes measured from PTR-MS are composed of *d*-limonene and α-pinene with a ratio of 1:1 based on the anthropogenic origins of monoterpene, as discussed in text S2. [b] The parameters were assumed to be equal to that of phenol.

3 Results and Discussion

3.1 Quantification and chemical composition of oxidized organic nitrogen

Fig. 1a shows a subset of the time series of pOON measured using the CIMS (i.e., $pOON_{CIMS}$) and $pOrgNO_{3,AMS}$ (-ONO_2 + NO_2 group) measured with the AMS. Total OA measured with the AMS is also shown in Fig. 1a. During the entire campaign, a moderate correlation (Pearson correlation coefficient, R = 0.42) was observed between $pOON_{CIMS}$ and $pOrgNO_{3,AMS}$ (Fig. 1b), which is probably due to the high uncertainty of $pOrgNO_{3,AMS}$ estimation from the AMS when organic nitrate fraction in total nitrate signal is low (<10%, the details can be found in Text S1), as well as is probably due to the fact that only –ONO_2/NO_2 groups not entire ON molecule was measured with AMS. The description of the correlation coefficient (R) within this study is defined based on the interpretation by Dancey and Reidy (2007), as shown in detail in Text S1. When the mass concentration of total nitrates from the AMS is below 5 μg m^{-3} (corresponding to $pOrgNO_{3,AMS}$ signal fraction in total nitrate signal >60%), an improved correlation between $pOON_{CIMS}$ and $pOrgNO_{3,AMS}$ is found (R = 0.86, Fig. 1b and Fig. S5), validating the robustness of $pOON_{CIMS}$ measured here. A similar moderate correlation between $pOrgNO_{3,AMS}$ and $pOON_{CIMS}$ was also observed at a rural site in the southwest Germany (R = 0.52) (Huang et al., 2019), and a much better agreement (R = 0.82) was obtained in the southeast US when the $pOrgNO_{3,AMS}$ fraction in total nitrate is above 70% (Lee et al., 2016; Xu et al., 2015).

https://doi.org/10.5194/acp-2023-8
Preprint. Discussion started: 16 January 2023
© Author(s) 2023. CC BY 4.0 License.

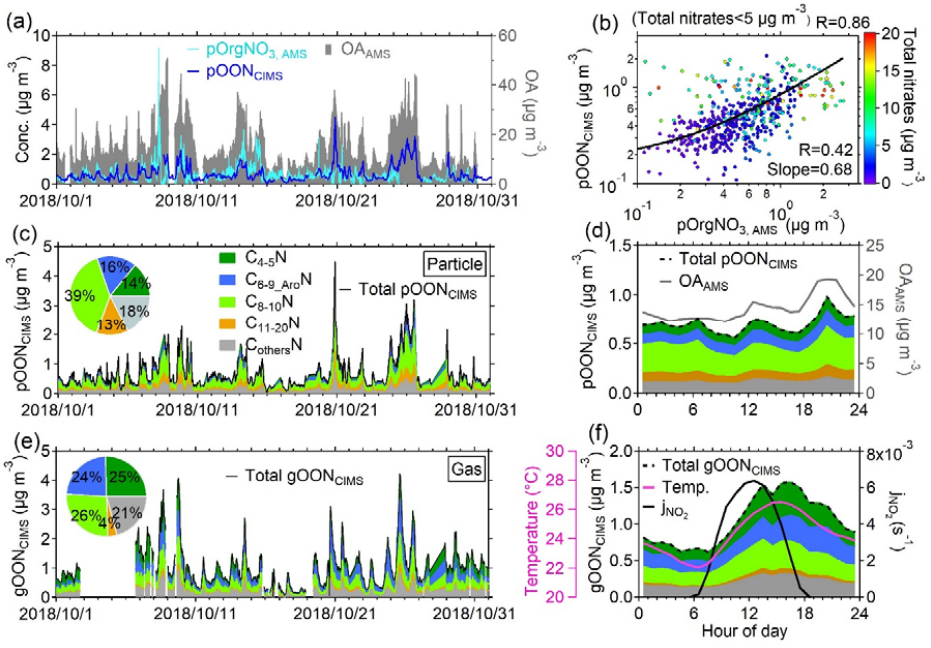

Figure 1. Time series and variations of OON during the PRIDE-GBA campaign. (a) Time series of $pOON_{CIMS}$ and $pOrgNO_{3,AMS}$. Time series of total OA detected by the AMS is shown on the right axis. (b) Scatterplot of $pOON_{CIMS}$ versus $pOrgNO_{3,AMS}$ during the campaign. The term "total nitrates <5 μg m^{-3}" indicates that the mass concentration of total nitrates (including organic nitrate and inorganic nitrate) measured by the AMS is lower than 5 μg m^{-3}. The points are color-coded using the total nitrate signals measured by the AMS. The logarithm was applied for both of the axes. The corresponding joint histogram plot can be found in Fig. S5. Time series of (c) $pOON_{CIMS}$ and (e) $gOON_{CIMS}$, as well as the time series of their C_xN groups from the CIMS measurement. The insets show their average mass contributions to total $gOON_{CIMS}$ and $pOON_{CIMS}$ during the campaign, respectively. The average diurnal variations of (d) $pOON_{CIMS}$ and its C_xN groups, as well as OA; (f) Average diurnal variations of total $gOON_{CIMS}$ and its C_xN groups, photolysis rate of NO_2 (j_{NO2}), and temperature during the entire campaign. All the diurnal variations calculated throughout the manuscript are based on the average values. All the linear fitting are based on the orthogonal distance regression (ODR) algorithm in this study.

The average concentrations of the $gOON_{CIMS}$ and $pOON_{CIMS}$ measured using the CIMS were 1.00 ± 0.67 and 0.66 ± 0.53 μg m^{-3}, respectively. Moreover, an average concentration of 0.60 ± 0.46 μg m^{-3} for $pOrgNO_{3,AMS}$ during the campaign was obtained. Notably, different size cuts between the AMS (PM_1) and the CIMS ($PM_{2.5}$) should only play a minor role in the quantification of pOON, as the measured total aerosol mass concentrations of $PM_{2.5}$ and PM_1 during the campaign are very similar (a regression slope of 0.96) (Chen et al., 2021a). The average mass-weighted chemical compositions for $gOON_{CIMS}$ and $pOON_{CIMS}$ observed in this campaign were determined to be $C_{6.6}H_{9.4}N_{1.1}O_{5.3}$ and $C_{8.5}H_{12.2}N_{1.1}O_{6.5}$, respectively, corresponding to molecular weight (MW) of 189 ± 7.8 and 234 ± 7.9 g mol^{-1}. The molecular weight of $pOON_{CIMS}$ in this study (234 ± 7.9 g mol^{-1}) is slightly lower than the

https://doi.org/10.5194/acp-2023-8
Preprint. Discussion started: 16 January 2023
© Author(s) 2023. CC BY 4.0 License.

Atmospheric Chemistry and Physics Discussions

reported values in forest (256 g mol^{-1}) and rural (296 g mol^{-1}) sites (Lee et al., 2018; Huang et al., 2019). If such average MW of pOON$_{CIMS}$ was applied,the pOON$_{AMS}$ (in addition to $-ONO_2$/-NO_2 groups, the organics part was also accounted for) would be 2.3 μg m^{-3} based on multiplying a factor of 3.8 to pOrgNO$_{3,\ AMS}$, which is well within the range of 0.06–2.94 μg m^{-3} of pOON$_{AMS}$ as reported in the previous studies around the world, as shown in Fig. S6. On the other side, if only $-ONO_2$/-NO_2 groups are considered to calculate pON$_{CIMS}$ to be pOrgNO$_{3,\ CIMS}$, the calculated pOrgNO$_{3,\ CIMS}$ can explain ~28% of pOrgNO$_{3,\ AMS}$, which is consistent with the fraction (23%) of total functionalized OA detected using the CIMS versus total OA measured using the AMS (Ye et al., 2021).

For this study, an average mass fraction of 15% of pON$_{AMS}$ in total OA (14.7 μg m^{-3} on average) based on AMS data was observed (calculation method referred to Takeuchi and Ng (2019)). In spite of the absolute mass concentrations of pON varied largely in different studied urban environments, the pON/OA ratios are very similar (15 ± 3% on average, Fig. S6), suggesting a potential similar pON formation process/fate in the urban areas (Day et al., 2010; Rollins et al., 2012; Xu et al., 2015).

To further illustrate the contributions of different components of speciated gOON and pOON measured by the CIMS, five C_xN groups, namely (1) $C_{4-5}N$, (2) $C_{6-9\ Aro}N$, (3) $C_{8-10}N$, (4) $C_{11-20}N$, and (5) $C_{others}N$ (Figs. 1c and 1e) were categorized only based on the number of carbon atoms in the molecules. The $C_{6-9\_Aro}N$ group was recognized based on the number of 6–9 carbon atoms and positive aromaticity index (0–1) (Text S4) (Koch and Dittmar, 2016; Wang et al., 2019; Koch and Dittmar, 2006). $C_{11-20}N$ group contains species with large carbon backbones from 10 to 20 and/or oligomers, $C_{others}N$ includes the remaining nitrogen-containing short-chain ions which are not possible to fit into the previous four categories, such as the ions with carbon atoms less than 4 (e.g., $C_3H_7NO_4$ and $C_3H_7NO_5$) and the ions with 6–9 carbon atoms excluded in $C_{6-9\ Aro}N$ group (e.g., $C_6H_9NO_3$ and $C_7H_{11}NO_5$). In general, it is observed that the contributions of $C_{4-5}N$ (25%) and $C_{6-9\ Aro}N$ (24%) to total gOON are higher than those to total pOON (14% and 16%, respectively), while $C_{8-10}N$ (39%) and $C_{11-20}N$ (13%) contributed more to total pOON than to total gOON (26% and 4%, respectively). These results are consistent with the lower volatility for $C_{8-10}N$ and $C_{11-20}N$ than those for $C_{4-5}N$ and $C_{6-9\ Aro}N$ due to the longer backbones of compounds in the former groups (Kroll and Seinfeld, 2008; Odum et al., 1996). In general, the time series of all groups for the gOON shows similar variability as the pOON (correlation coefficient $R > 0.6$), except for $C_{4-5}N$ groups that show a positive correlation of $R = 0.31$ (Fig. S7). The slightly poor correlation of $C_{4-5}N$ groups between gas and aerosol phase was probably caused by their high susceptibility influenced by temperature. The regression slope between gOON and pOON of each category (3.61 to 1.80) decreases with the increase of the carbon number, as shown in Fig. S7, which is reasonable considering their gas/particle partitioning balances (Odum et al., 1996).

https://doi.org/10.5194/acp-2023-8
Preprint. Discussion started: 16 January 2023
© Author(s) 2023. CC BY 4.0 License.

Atmospheric Chemistry and Physics Discussions

The overall average diurnal variations of gOON and pOON and their C_xN groups are shown in Figs. 1d and 1f. Despite the boundary layer expansion in the daytime (Fig. S8a), the gOON peaks in the afternoon and drops slowly with tail toward the night. The enhancement of the gOON increases with the photolysis rate (Fig. 1f), indicating that daytime secondary formation is an important source of gOON (Sobanski et al., 2017). The primary biomass burning (e.g., levoglucosan as a tracer) and vehicle emissions (e.g., NO/NO_x as tracers), which are also potential sources for gOON, usually show enhancement during nighttime (levoglucosan in Fig. S10f and NO/NO_x in Fig. S8b) and morning rush hour time (NO/NO_x only), respectively, in their diurnal variations, indicating that both primary sources are unlikely to contribute to the gOON enhancement during daytime. In contrast to the gOON, the pOON exhibits two peaks during the afternoon and nighttime (Fig. 1f), indicating the possibility of different sources and formation mechanisms for the pOON compared to the gOON, e.g., biomass burning contribution during nighttime (Rollins et al., 2012). A more detailed analysis about the sources of the gOON and pOON is presented in the next section.

In general, the average diurnal concentration of each gOON (pOON) group shows a similar trend (Figs. S8d and S8g). The fraction of $C_{4-5}N$ group in gOON enhances slightly during daytime (Fig. S8e), which might be due to strong photochemical formation of isoprene-nitrates (Fisher et al., 2016; Reeves et al., 2020; Mayhew et al., 2022; Hamilton et al., 2021). The $C_{8-10}N$ fraction in total pOON slightly enhances during nighttime (Fig. S8h), which was probably due to the primary emissions and the formation of monoterpene-nitrates by NO_3 oxidation chemistry (Peng et al., 2021; Fisher et al., 2016).

3.2 Source apportionment of oxidized organic nitrogen.

To elucidate the sources of OON measured using the CIMS, the correlations between OON and a wide range of trace species representing different sources were explored to filter the best tracer for source apportionment. The scatterplots of gOON and pOON (hereinafter represent the $gOON_{CIMS}$ and $pOON_{CIMS}$) with selected species, including particle-phase levoglucosan ($C_6H_{10}O_5$) measured using the CIMS; *m/z* 60 measured using the AMS, benzene, NO_x, and CO are shown in Fig. 2 and Fig. S9. It was observed herein that the scatterplots of gOON (and pOON) versus levoglucosan, a tracer for biomass burning emissions (Li et al., 2021b; Simoneit, 2002; Simoneit et al., 1999), exhibit two different regression slopes during daytime and nighttime (Figs. 2a and 2c). However, different regression slopes were not observed in the scatterplots of OON versus other tracers, e.g., CO, benzene. It suggests the biomass burning which usually peaks during the night might be important source for OON. The time series of OON, in particular pOON, indeed peak consistently with levoglucosan during high concentration episodes (Figs. S11a and S12a), indicating biomass burning emissions contributed substantially to OON during this campaign. For other biomass burning tracer, e.g., *m/z* 60, did not show separated regression slope with OON, which is probably due to elevated background of *m/z* 60 contributed by non-biomass burning emissions (Cubison et al., 2011; Mohr et al., 2009). Another two biomass burning tracers, i.e., methoxyphenol

https://doi.org/10.5194/acp-2023-8
Preprint. Discussion started: 16 January 2023
© Author(s) 2023. CC BY 4.0 License.

Atmospheric Chemistry and Physics Discussions

and vanillic acid, the former of which exhibits relatively low concentration and the latter shows larger background than levoglucosan (Fig. S10), are both not the ideal biomass burning tracers in this study.

In contrast to that levoglucosan and OON peak consistent with each other, the time series of OON did not peak during the episodes with strong influences of vehicle emissions (as indicative of high NO/NO_x concentration >50 ppb) (Harrison et al., 2003; Wormhoudt et al., 2015) , as shown in Figs. S13a and S14a. In addition, the anti-correlations between OON and NO/NO_x during some of these episodes were even found, indicating that vehicle emission is not a significant source of primary OON. Furthermore, it was found that the diurnal variation of pOON peaks one-hour earlier than NO_x in the morning time, thus, supports their different origins (Fig. S14g). The coincidence peaking time between pOON and NO_x during nighttime is probably more influenced by biomass burning. Another piece of evidence is that multiple laboratory studies found negligible emission of gOON from emission tests of vehicle exhaust based on Iodide-CIMS direct measurement (Le Breton et al., 2019; Li et al., 2021a). Thus, the biomass burning emissions and secondary formation should be the main sources of OON observed in this campaign.

To quantify the contributions of biomass burning (OON_{bb}) and secondary formation (OON_{sec}) to OON in both gas and particle phases, the following Eqs. (1) and (2) was proposed to allocate the OON sources:

$$OON_{bb} = ([OON_{measured}]/[levo.])_{bb} \times [levo.] \quad (1)$$

$$OON_{sec} = OON_{measured} - OON_{bb} \quad (2)$$

Where [levo.] is the concentration of particulate levoglucosan measured using the CIMS, $([OON_{measured}]/[levo.])_{bb}$ is the averaged ambient concentration ratio determined from slopes between ambient OON and particulate levoglucosan during selected episodes with strong influences of biomass burning (Figs. S11 and S12). This approach relies on the concept similar to the widely-used "elemental carbon tracer method" for source apportionment of primary and secondary organic carbon (Turpin and Huntzicker, 1995). A similar method was used by Salvador et al. (2021) to quantify the sources of nitro-aromatic compounds. The episodes were selected based on the following three criteria: (1) the peak concentration of levoglucosan should be above 0.2 μg m^{-3} for selecting periods strongly influenced by biomass burning plumes; (2) the regression coefficient R between gOON (pOON) and levoglucosan during each episode should be >0.7; and (3) the number of the fitting points during each episode should be above 4, due to the hourly data of particle-phase levoglucosan were used. The averaged ambient concentration ratios were determined to be 3.95 ± 1.67 μg m^{-3}/μg m^{-3} for gON and 5.05 ± 1.01 μg m^{-3}/μg m^{-3} for pOON, as presented in Table S1. The variability of $[OON_{measured}]/[levo.]$ ratios from multiple biomass burning episodes for pOON is 20%. The slightly larger ratio uncertainty for gOON (42%) is mainly due to active gas-phase reaction and low contributions of biomass burning emissions to total gOON, as discussed below.

https://doi.org/10.5194/acp-2023-8
Preprint. Discussion started: 16 January 2023
© Author(s) 2023. CC BY 4.0 License.

Atmospheric Chemistry and Physics Discussions

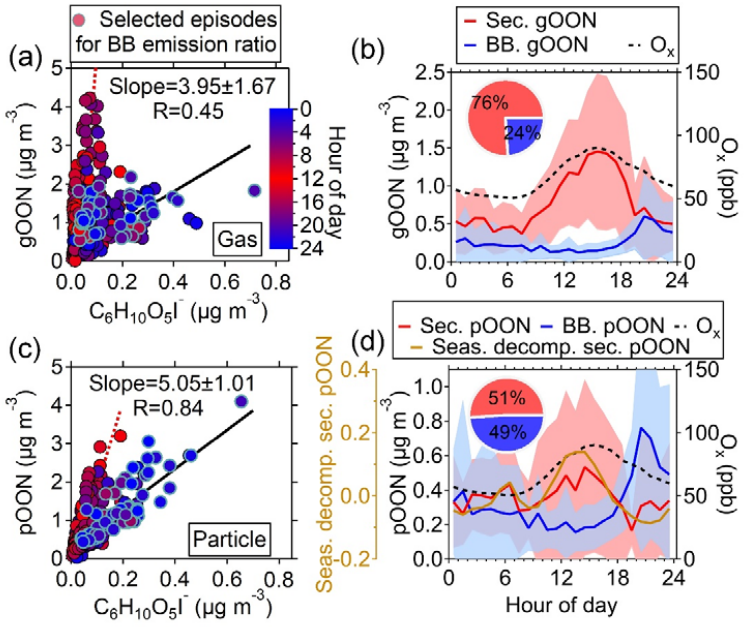

Figure 2. Scatterplots of (a) gOON and (d) pOON versus levoglucosan with the data points color-coded using hour of day. The blue circles indicate the data points from multiple strongly influenced episodes by biomass burning emission, of which the ratios between gOON or pOON and levoglucosan were used to determine the average ratio (black regression line). The red dotted line means the line regression during the daytime. The diurnal variations of (b) gOON and (e) pOON from biomass burning (BB.) and secondary formation (sec.). The shaded areas mean the standard deviations. The seasonal decomposed secondary pOON (Text S4) and O_x are also shown. The inset pies are the contributions from biomass burning and secondary formation to total gOON and pOON, respectively.

The ratios, i.e., $([OON_{measured}]/[levo.])_{bb}$, were obtained based on ambient measurement; therefore, the ratios might be influenced by secondary formation within biomass burning plumes, thus the OON_{bb} herein is referred to as the total primary and secondary OON concentration from biomass burning emissions. OON_{sec} is defined as secondary OON from other non-biomass burning sources, e.g., biogenic and non-biomass burning anthropogenic sources. By using this approach, the estimated diurnal variation and time series of OON from biomass burning (OON_{bb}) and secondary formation (OON_{sec}) are shown in Figs. 2 and 3. Compared with the measured total OON, the OON_{sec} exhibit better agreement with the total gOON production rate in terms of both time series and correlation coefficients (R increases from 0.61 to 0.65 for gOON, and 0.19 to 0.45 for pOON, Fig. S15) In particular, better agreement was found during 24–26 October 2018 when the contributions of biomass burning to OON are high. These results validated the source apportionment of OON applied herein.

https://doi.org/10.5194/acp-2023-8
Preprint. Discussion started: 16 January 2023
© Author(s) 2023. CC BY 4.0 License.

Atmospheric Chemistry and Physics Discussions

On average, biomass burning emissions accounted for 49 ± 10% of total pOON, while the contribution was much lower (24 ± 11%) for gOON (Figs. 2b and 2d), indicating that biomass burning is one of the major sources for pOON, and gOON is predominately from secondary formation (~76%) (Huang et al., 2019; Lee et al., 2016). The high contribution of biomass burning to total pOON is consistent with the results of relevant previous studies (Mohr et al., 2013; Wang and Li, 2021; Wang et al., 2017b; Wang et al., 2019), in which substantial OON compounds were observed in biomass burning plumes. In this study, the nighttime enhancement of levoglucosan indicates that the influence of biomass burning at this site was mainly contributed by the plumes of the agricultural residue combustion transported from the vicinity of Guangzhou city, as shown in the MODIS wildfire point plot in Fig. S16 (Wang L.J et al., 2017; Yuan et al., 2010). Moreover, the ambient ratio of levoglucosan to water-soluble potassium (K^+) (0.20 ± 0.04) observed in this study also supports that the biomass burning at this site was contributed by the combustion of crop residuals (0.1–0.2) rather than wood combustion (5.8–24.0) (Cheng et al., 2013). Fig. S17 presents the Van Krevelen diagram of all OON compounds in this study. The appearance of OON compounds observed herein is linked with both fresh and aged biomass burning emissions (Wang et al., 2019). In general, most of the biomass burning OON were found in particle phases, indicating that the OON formed in biomass burning plumes have generally lower volatility than OON formed via O_3, NO_3 oxidation, or OON oxidized from non-biomass burning related precursors.

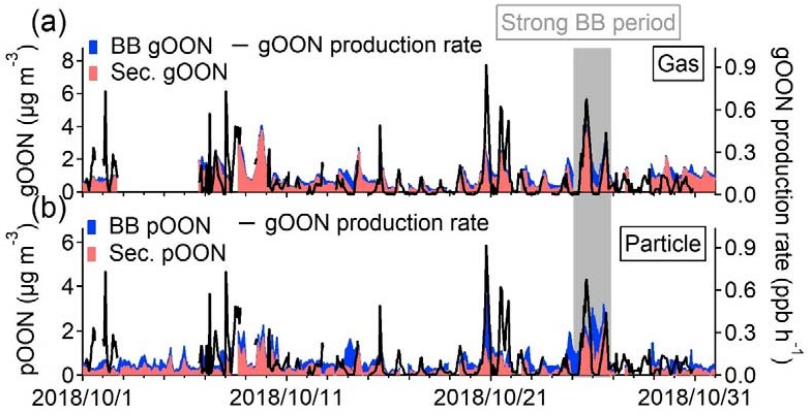

Figure 3. Stacked time series of secondary and biomass burning (a) gOON, (b) pOON. The gON production rate is presented on the right axis in both of the figures. The grey period represents a strong biomass burning emission period during 24−26 October 2018, which was selected based on the high mass concentrations of levoglucosan and other biomass burning tracers in their time series in Fig. S10.

Based on the diurnal pattern, secondary gOON peaks during the afternoon (1.49 ± 0.49 μg m^{-3}), which is consistent with the peaking time of O_x ($[O_x] = [O_3] + [NO_2]$), and then reduces rapidly to 0.43–0.83 μg m^{-3} at night (Fig. 2b). The similar averaged

https://doi.org/10.5194/acp-2023-8
Preprint. Discussion started: 16 January 2023
© Author(s) 2023. CC BY 4.0 License.

Atmospheric Chemistry and Physics Discussions

diurnal variations of gOON and O_x indicate that the daytime chemistry corresponds to the major formation pathway of gOON. Secondary pOON also shows a slight peak (0.39 ± 0.07 μg m^{-3}) corresponding to O_x during daytime, however, exhibits much larger uncertainty than the secondary gOON. To elucidate this large uncertainty, a seasonal decomposition method, which can down weight the impact of daily peak intensity variation, was applied (detailed process can be found in Text S4). Clear diurnal variation of secondary pOON after seasonal decomposition is displayed in Fig. 2d, which supports the daytime peak of secondary pOON. During nighttime, the concentration of pOON (0.32 ± 0.07 μg m^{-3}) remains at a high level with a peak at 6 o'clock (Fig. 2d), indicating that there is a different formation pathway or formation yield for secondary pOON compared to secondary gOON at night. It is speculated that the enhanced secondary pOON formation at night is probably associated with higher yield of pOON from NO_3 chemistry, as well as heterogeneous reactions of NO_3 and N_2O_5 at particle surface, which is discussed in detail in the following section. Following Eqs. (1) and (2), the averaged concentration ratios for each category of particle-phase C_xN (pC_xN) were also calculated separately, thus the contributions of biomass burning and secondary formation for each pC_xN group were estimated (Fig. S18). The contribution from biomass burning to each pC_xN group only show small difference, ranging from 52% for the $C_{6-9\ Aro}N$ group to 40% for the $C_{4-5}N$ group, indicating biomass burning is an important source for OON at wide carbon numbers.

3.3 Secondary formation pathways of oxidized organic nitrogen.

To further elucidate the secondary formation mechanism of gOON, the diurnal patterns of gOON production rates from the three pathways following the procedure mentioned in section 2.3 are shown in Fig. 4a and Fig. S19. As expected, the gOON production rates from OH- and O_3-initiated oxidation peaking (0.14 ppb h^{-1} and 0.01 ppb h^{-1}, respectively) at noon (11:00–13:00) are due to the high concentrations of these two oxidants during this period (3.9×10^6 and 1.4×10^8 molecule cm^{-3}, respectively) (Wang et al., 2020c). Interestingly, the gOON production rate from NO_3-initiated oxidation peaks at around 0.10 ± 0.18 ppb h^{-1} from late afternoon to evening (16:00–19:00, Fig. 4a). This is mainly due to the high NO_3 concentration (2.08 ± 1.32 ppt, Fig. S3d) when the low NO (1.37 ± 0.34 ppb) and moderate O_3 (53 ± 34 ppb) and NO_2 (31 ± 13 ppb) (Fig. S8b) concentrations appear during that period of the day. The precursors, i.e., cresol, phenol, isoprene, and monoterpenes, do not show rising concentrations during the period (16:00–19:00) except for some aromatics (Figs. S8c, S8f, and S8i), indicating that not the precursor VOCs but the high NO_3 concentration is the main contributor for this enhancement of NO_3-initiated gOON production rate during the day. The inconsistent peaks for the secondary gOON production rate and secondary gOON mass loading may be due to the (i) counteraction of photochemical formation and degradation, and or (ii) effect of survivor bias from measured VOCs (Wang et al., 2022b; Perring et al., 2013).

In general, OH- and NO_3-initiated oxidation pathways dominated the secondary gOON formation in this study and accounted for 42% and 49% of total gOON production rate, respectively, while the remaining was attributed to the O_3-initiated

https://doi.org/10.5194/acp-2023-8
Preprint. Discussion started: 16 January 2023
© Author(s) 2023. CC BY 4.0 License.

Atmospheric Chemistry and Physics Discussions

oxidation pathway (9%). Fig. S19 shows that the contribution to total gOON production rate from 8:00 to 14:00 mainly came from OH chemistry (73%), then quickly changed to NO_3 chemistry during the late afternoon (mean 55%) and onward (mean 86% at night). These results emphasize the importance of NO_3 chemistry for the gOON production rate during later daytime and the entire night in this urban area. The importance of NO_3 chemistry toward ON formation was also found in other locations. For example, high contributions of NO_3 chemistry to secondary gOON production rate in Finnish boreal forest (41% during the day and almost 100% at night) (Liebmann et al., 2019) and isoprene-derived gOON production rate in Beijing urban area (32% in the afternoon and 86% at nighttime) (Hamilton et al., 2021) were observed. The low contribution of O_3 pathway (9%) at this site is also consistent with the estimated fraction (12%) at a forest area (Liebmann et al., 2019).

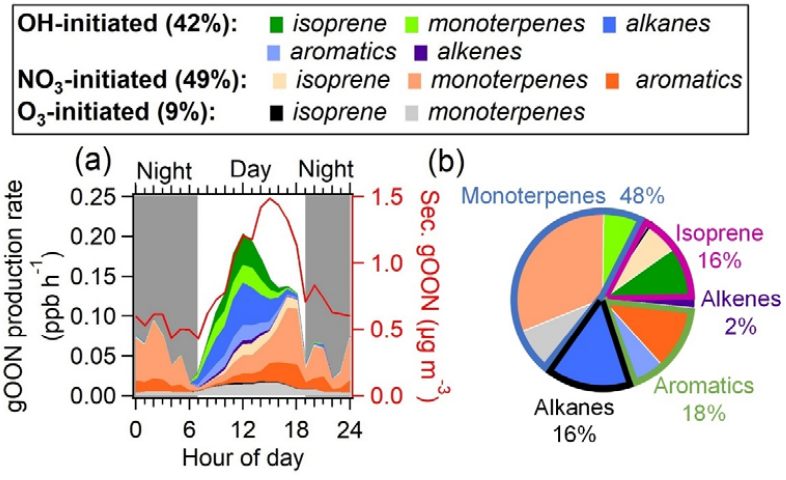

Figure 4. (a) Average diurnal variations of categorized gOON production rates and the concentration of secondary gOON for the whole campaign. (b) Contributions of various VOC precursors to total gON production rate.

Fig. 4b displays the contributions to the gOON production rate from different VOC precursors, among which monoterpenes account for 48% of total gOON production rate. The remaining contribution is attributed to biogenic VOC, i.e., isoprene (16%), and other anthropogenic VOCs including aromatics (18%), alkanes (16%), and alkenes (2%). These results indicate that monoterpenes are the largest contributor to the secondary formation of multifunctional gOON in this urban region. Relatively high concentrations of monoterpenes were observed during the campaign (mean: 0.14 ± 0.14 ppb; range: 0.003–1.5 ppb). Strong correlations of the daily-averaged values from nighttime monoterpenes with two tracers of volatile chemical product (VCP) sources (C8 aromatics, R = 0.85 and ethanol, R = 0.78), and moderate correlation with CO (R = 0.62) as well as biomass burning tracer levoglucosan (R = 0.50) (Fig. 5) were also found. These strong and moderate correlations with monoterpene are in contrast with the poor correlations of these anthropogenic tracers with biogenic-derived isoprene during daytime (R = –0.09 to 0.20, Fig. S20). The ambient ratio of

https://doi.org/10.5194/acp-2023-8
Preprint. Discussion started: 16 January 2023
© Author(s) 2023. CC BY 4.0 License.

Atmospheric Chemistry and Physics Discussions

monoterpenes to CO (1.82 ppb ppm^{-1}) determined in Fig. 5c is significantly higher than their emission ratios from vehicle exhausts (0.001–0.35 ppb ppm^{-1}) (Wang et al., 2022a). Combining these results, it is concluded that the monoterpenes observed during this campaign should be mainly of anthropogenic origin (Hellén et al., 2012), with VCPs as the potentially most important source. Recent studies in the US also demonstrated that monoterpenes are strongly emitted by the VCP sources in highly populated areas (Coggon et al., 2021; Gkatzelis et al., 2021). In addition, a field study conducted in the tower located in Guangzhou urban area found the ambient monoterpenes at altitude of 450 m are predominantly come from VCP sources (Li et al., 2022), which is consistent with the findings here. As a result, considering monoterpenes of anthropogenic origin, anthropogenic VOCs accounted for 80% of total gON production rate. Note that certain contributions of biogenic-derived monoterpenes might offset the anthropogenic-origin OON; however, other anthropogenic VOCs, such as long-chain or cyclic alkanes/alkenes (Wang et al., 2020a; Zhao et al., 2016), which are important precursors for OONs in urban areas (Lee et al., 2015; Lim and Ziemann, 2009; Matsunaga and Ziemann, 2010), were not considered herein due to the omission of data. Thus, anthropogenic contribution to the gON estimated via secondary gON production rates might be biased low.

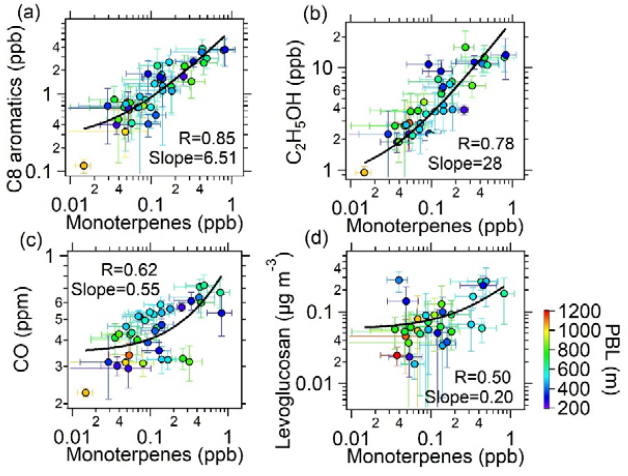

Figure 5. Scatter plots between the averaged concentrations of (a) C8 aromatics, (b) ethanol, (c) CO, and (d) levoglucosan versus monoterpenes at night (19:00−6:00 next day) during the entire campaign. The color represents the planetary boundary layer height (PBL). The error bars were the standard deviations of average values during nighttime. The logarithm was applied for both of the axes.

Fig. 6a shows a strong correlation between secondary gOON and O_x (R = 0.83, slope = 0.02 μg m^{-3}/ppb), which is within expectation as the major channel of gOON formation between peroxy radicals (RO_2) and NO can lead to the formation of O_3 by continual radical propagation and photolysis of NO_2 (Perring et al., 2013). Fig. 6b demonstrates that secondary pOON shows moderate correlation (R = 0.39) with O_x and secondary pOON/O_x ratio increases as a function of RH (from ~0.002 to ~0.03 μg m^{-}

https://doi.org/10.5194/acp-2023-8
Preprint. Discussion started: 16 January 2023
© Author(s) 2023. CC BY 4.0 License.

Atmospheric Chemistry and Physics Discussions

^{3}/ppb), aerosol liquid water content (ALWC) (Fig. S21b) and wet aerosol surface area (Fig. S21c). The elevated RH and ALWC may lead to an increase in the aerosol surface area to facilitate more highly functionalized and water-soluble gOON partitioning into particle phase and/or to promote NO_2, NO_3, and/or N_2O_5 uptake onto aerosol phase (George et al., 2015; George and Abbatt, 2010). Moreover, aerosols become more liquified at higher RH, thus leading to the increase in molecular diffusion in aerosols to promote heterogeneous reactions (George et al., 2015) of NO_3 with unsaturated species (Xiao and Bertram, 2011; Zhao et al., 2011), NO_2 with aromatic species, and N_2O_5 with alcohols to form pOON (Gross et al., 2009; Lee et al., 2015). Indeed, lower gas/particle partitioning coefficient (saturation mass concentration, C^*) of OON at RH >70% than low RH (<70%) was found, (Fig. S22a), which supports the favored pOON formation from heterogeneous reactions. A study in an anthropogenic-emission-dominated region also showed the heterogeneous reactions through N_2O_5 uptake can explain around half of the formation of particle-phase alkyl nitrates (Lee et al., 2015), thus signifying the important contribution from heterogeneous reactions to pOON. The secondary pOON/O_x ratio shows much worse correlation with temperature (Fig. S21d), indicating that lower temperature-induced higher partition to particles contributes little to higher pOON during nighttime.

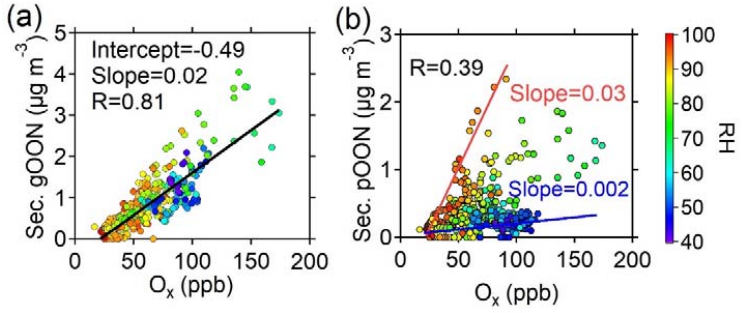

Figure 6. Scatterplots of (a) secondary gOON and (b) secondary pOON versus O_x color-coded using RH during the campaign. The red and blue lines are plotted for guiding eyes.

Furthermore, the lifetime of gON in this study was calculated based on the correlation between secondary gOON and the secondary gON production rate (Liebmann et al., 2019) as shown in Fig. S22b. The roughly estimated lifetime of gON is around 0.54–0.78 h during daytime and nighttime, respectively, which is shorter than the lifetime of alkyl nitrates (~2 ± 3 h) found in the boreal forest (Liebmann et al., 2019). This might be associated with the stronger photolysis, oxidative degradation, and different chemical composition of gON in urban area compared to boreal forest (Perring et al., 2013). The incomplete measurement of gON by the CIMS was one of the potential reasons as well. For the lifetime of pON, a modeling study including explicit formation mechanism as conducted in Lee et al. (2016) is required for systematic explorations in the future.

https://doi.org/10.5194/acp-2023-8
Preprint. Discussion started: 16 January 2023
© Author(s) 2023. CC BY 4.0 License.

Atmospheric Chemistry and Physics Discussions

3.4 Molecular chemical compositions of oxidized organic nitrogen.

In this section, the molecular components of the gOON and pOON categorized with different oxygen and carbon atom numbers are briefly discussed. Fig. 7 shows the overview of the distribution of molecular OON during the entire campaign, as well as secondary-dominated period for gOON and biomass burning-dominated period for pOON. In general, the gOON abundance is dominated by C_5-C_8 and C_{10} compounds (65–70%), while the pON shows peaks around C_8 and C_{10} compounds. The highly oxidized molecules (containing at least 6 oxygen atoms) contributed 44% and 71% to gOON and pOON, respectively. By comparing the ion distribution of total gOON in the whole campaign versus in the period dominated by secondary sources (Fig. 7a), we found that the mass concentration fraction of C_4 compounds in total gOON is much enhanced, while C_6 and C_{10} compounds are significantly decreased. The enhanced C_4 compounds (e.g., $C_4H_7NO_5$ as the most abundant ion in gON, Fig. S17) are probably contributed by the isoprene oxidation during the day (Wennberg et al., 2018; Brownwood et al., 2021). The decreases of C_6 and C_{10} compounds in gON during secondary-dominated period indicate a large fraction of these compounds might come from biomass burning sources. For example, $C_6H_5NO_3$ (nitrophenol) in C_6 is the second most (7.4%) abundant compounds in gOON. Multiple ambient studies had shown that biomass burning emission can contribute substantially to $C_6H_5NO_3$ (Mohr et al., 2013; Wang et al., 2018), e.g., 58% in Beijing (Song et al., 2021), consistent with the finding shown here.

The almost identical distributions of pOON during the whole campaign and biomass burning-dominated period mainly result from approximate contributions from biomass burning (49% and ~70%, respectively). The C_{10} compounds contribute both high (~22%) in pOON during the whole campaign and biomass burning-dominated period (biomass burning contribution of pOON > 60%, Fig. S23b), confirming the important contribution of biomass burning to this type of compounds (Figs. 7b). In pOON, the abundance of $C_{10}H_xNO_y$ ($y \geq 6$) in pOON (19%) is higher than that in gOON (9%), which is reasonable due to their low volatility with multiple functional groups (Odum et al., 1996). The good correlations of the time series between $C_{10}H_xNO_y$ ($y \geq 6$) ions and the biomass burning tracer levoglucosan ($0.52 < R < 0.79$) suggested these ions indeed mainly come from emission or oxidation processes within biomass burning plumes. The extremely oxidized C_{10} compounds (containing at least 8 oxygen atoms) might come from multiple oxidation steps and autoxidation mechanism (Iyer et al., 2021; Zhao et al., 2018; Pye et al., 2019; Shen et al., 2021; Mayorga et al., 2022), demonstrating that the complex secondary formation processes indeed happened within the biomass burning plumes. There are high mass peaks at the positions corresponding to C_{16} and C_{20} species in pOON (Figs. 7b), which are oligomers. These ions might come from direct emission and/or oxidation process in biomass burning plumes, e.g., dimerization of C_8 and C_{10} species (Wu et al., 2021; Lee et al., 2018).

https://doi.org/10.5194/acp-2023-8
Preprint. Discussion started: 16 January 2023
© Author(s) 2023. CC BY 4.0 License.

Atmospheric Chemistry and Physics Discussions

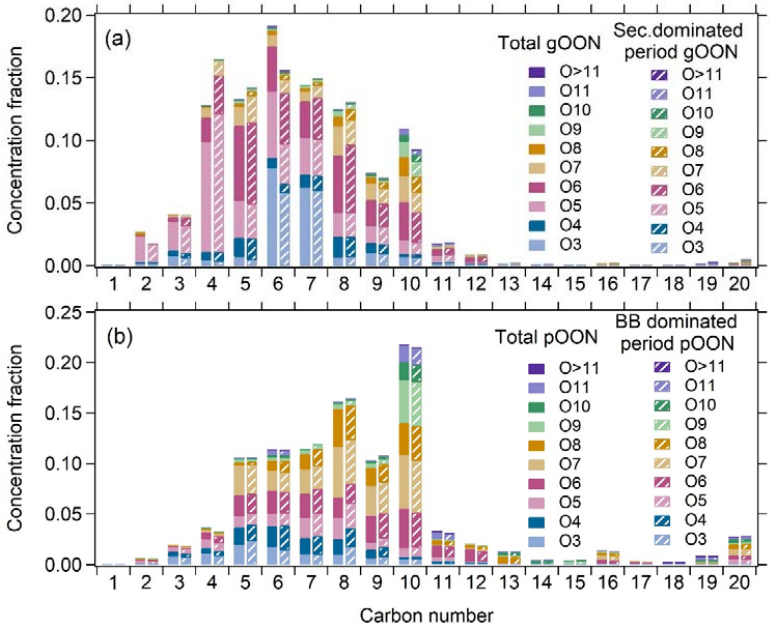

Figure 7. Concentration fractions of (a) gOON categorized based on carbon numbers and oxygen numbers during the whole campaign and the secondary (sec.) formation-dominated period (13:00−15:00) (Fig. S23a). Similar plot is displayed for (b) pOON during the whole campaign and the biomass burning (BB) dominated period (19:00−21:00) (Fig. S23b).

4 Conclusions

The mass concentrations, sources, and formation mechanism of gas- and particle-phase OON were systematically investigated in a megacity in the southern China. The good comparison of pOON measured by AMS and FIGAERO-CIMS indicates that the CIMS can measure a fraction of ~28% of total pOON in this study. The missed pOON mass is probably due to the lack of detection of less-polar OON (keto/alkyl ON) and/or non-nitrogen-containing pOON resulting from the loss of $-NO_2$ group by thermal desorption in CIMS measurement.

Using levoglucosan as the biomass burning tracer for source apportionment, almost half of pOON is attributed to biomass burning in this study, underscoring the important contribution of biomass burning to pOON in this urban area. Biomass burning is a very common source across the world; The proposed estimation method in this study might help to clarify the exact biomass burning contribution to OON and their potential atmospheric implication. The gOON was mainly produced by secondary formation processes (76%), initiated by OH (42%) and NO_3 (49%) chemistry. The significant contribution of NO_3 chemistry to gOON and potentially to other secondary products, e.g., SOA, was not only observed in Guangzhou but also in the megacity of Beijing (Hamilton et al., 2021), highlighting the important daytime NO_3 chemistry in urban areas. This indicates that the importance of

https://doi.org/10.5194/acp-2023-8
Preprint. Discussion started: 16 January 2023
© Author(s) 2023. CC BY 4.0 License.

Atmospheric Chemistry and Physics Discussions

daytime NO_3 chemistry might not be unique and should be considered in other locations that are impacted by strong anthropogenic emissions. By ranking the precursors of OONs in the ambient atmosphere, monoterpenes are determined to be the most important VOC precursors for secondary gOON formation. Multiple evidences suggest that the monoterpene observed in study is anthropogenic-origins from VCP source. The monoterpene isomer measurement, which has seldomly been carried out in current Chinese urban areas, is highly recommended for future studies to evaluate the impact of biogenic and anthropogenic emissions (e.g., VCPs) on ozone and other secondary products in the ambient atmosphere.

Furthermore, in this study, it is also found that heterogeneous reactions might contribute substantially to the secondary formation of pOON in urban areas; however, the detailed mechanism and its quantified contribution to pOON in ambient air are still unclear, which warrants further investigation. A thorough comparison between modelled and measured pOON might shed light on this question. Highly functionalized gOON and pOON, as well as oligomers can be formed through multigenerational oxidation and autoxidation during biomass burning plumes, highlighting the complexity of sources and chemical processes in the urban environment. The results of this study provide valuable data and insights to understand the chemistry of reactive organic nitrogen in urban areas.

Data Availability

The data sets (Cai, 2022) used to evaluate the conclusions in the study are available at https://data.mendeley.com/datasets/s8s6wk32fy/1. Figures were made with Igor Pro version 6.37 and Igor Pro version 8.04, available under the Igor Pro license at https://www.wavemetrics.com. The more detailed data can be provided by contacting the corresponding authors.

Competing Interests

The authors declare no conflicts of interest relevant to this study.

Author contributions

YC and CY contributed equally to this work. YC and WH: writing, visualization, and validation; YC, CY, WC, WH, YP, BW, XH, LH, SG, and BY: data curation, methodology; CY, WC, WH, WS, YP, SH, JQ, SW, CW, CW, ZW, BY: experiment, investigation, and formal analysis; WH, BY, MS, and XW: conceptualization, supervision, project administration and funding acquisition.

https://doi.org/10.5194/acp-2023-8
Preprint. Discussion started: 16 January 2023
© Author(s) 2023. CC BY 4.0 License.

Atmospheric Chemistry and Physics Discussions

Acknowledgements

This work was supported by the National Natural Science Foundation of China (grant No. 41875156, 41877302, 41905111), Guangdong Pearl River Talents Program (2019QN01L948), Guangdong Foundation for Program of Science and Technology Research (Grant No. 2019B121205006), Guangdong Foundation for Program of Science and Technology Research (Grant No. 2020B1212060053), State Key Laboratory of Organic Geochemistry, GIGCAS (SKLOG2020−5, SKLOG2020−6). We would like to appreciate Joel A. Thornton and Brett B. Palm for their helpful comments.

Reference

Atkinson, R. and Arey, J.: Atmospheric Degradation of Volatile Organic Compounds, Chem. Rev., 103, 4605-4638, 10.1021/cr0206420, 2003.

Ayres, B. R., Allen, H. M., Draper, D. C., Brown, S. S., Wild, R. J., Jimenez, J. L., Day, D. A., Campuzano-Jost, P., Hu, W., de Gouw, J., Koss, A., Cohen, R. C., Duffey, K. C., Romer, P., Baumann, K., Edgerton, E., Takahama, S., Thornton, J. A., Lee, B. H., Lopez-Hilfiker, F. D., Mohr, C., Wennberg, P. O., Nguyen, T. B., Teng, A., Goldstein, A. H., Olson, K., and Fry, J. L.: Organic nitrate aerosol formation via NO3+ biogenic volatile organic compounds in the southeastern United States, Atmos. Chem. Phys., 15, 13377-13392, https://doi.org/10.5194/acp-15-13377-2015, 2015.

Bai, J., Sun, X., Zhang, C., Xu, Y., and Qi, C.: The OH-initiated atmospheric reaction mechanism and kinetics for levoglucosan emitted in biomass burning, Chemosphere, 93, 2004-2010, https://doi.org/10.1016/j.chemosphere.2013.07.021, 2013.

Bannan, T. J., Le Breton, M., Priestley, M., Worrall, S. D., Bacak, A., Marsden, N. A., Mehra, A., Hammes, J., Hallquist, M., Alfarra, M. R., Krieger, U. K., Reid, J. P., Jayne, J., Robinson, W., McFiggans, G., Coe, H., Percival, C. J., and Topping, D.: A method for extracting calibrated volatility information from the FIGAERO-HR-ToF-CIMS and its experimental application, Atmos. Meas. Tech., 12, 1429-1439, 10.5194/amt-12-1429-2019, 2019.

Bell, D. M., Wu, C., Bertrand, A., Graham, E., Schoonbaert, J., Giannoukos, S., Baltensperger, U., Prevot, A. S. H., Riipinen, I., El Haddad, I., and Mohr, C.: Particle-phase processing of α-pinene NO3 secondary organic aerosol in the dark, Atmos. Chem. Phys. Discuss., 2021, 1-28, 10.5194/acp-2021-379, 2021.

Bhattarai, H., Saikawa, E., Wan, X., Zhu, H., Ram, K., Gao, S., Kang, S., Zhang, Q., Zhang, Y., Wu, G., Wang, X., Kawamura, K., Fu, P., and Cong, Z.: Levoglucosan as a tracer of biomass burning: Recent progress and perspectives, Atmospheric Research, 220, 20-33, 10.1016/j.atmosres.2019.01.004, 2019.

Boyd, C. M., Sanchez, J., Xu, L., Eugene, A. J., Nah, T., Tuet, W. Y., Guzman, M. I., and Ng, N. L.: Secondary organic aerosol formation from the β-pinene+NO3 system: effect of humidity and peroxy radical fate, Atmos. Chem. Phys., 15, 7497-7522, https://doi.org/10.5194/acp-15-7497-2015, 2015.

Brown, S. S. and Stutz, J.: Nighttime radical observations and chemistry, Chem Soc Rev, 41, 6405-6447, 10.1039/c2cs35181a, 2012.

Brownwood, B., Turdziladze, A., Hohaus, T., Wu, R., Mentel, T. F., Carlsson, P. T. M., Tsiligiannis, E., Hallquist, M., Andres, S., Hantschke, L., Reimer, D., Rohrer, F., Tillmann, R., Winter, B., Liebmann, J., Brown, S. S., Kiendler-Scharr, A., Novelli, A., Fuchs, H., and Fry, J. L.: Gas-Particle Partitioning and SOA Yields of Organonitrate Products from NO3-Initiated Oxidation of Isoprene under Varied Chemical Regimes, ACS Earth Space Chem., 5, 785-800, 10.1021/acsearthspacechem.0c00311, 2021.

Cai, Y.: PRIDEGBA_Dataset [Dataset], Mendeley Data, V1, 10.17632/s8s6wk32fy.1, 2022.

Canagaratna, M. R., Jayne, J. T., Jimenez, J. L., Allan, J. D., Alfarra, M. R., Zhang, Q., Onasch, T. B., Drewnick, F., Coe, H., Middlebrook, A., Delia, A., Williams, L. R., Trimborn, A. M., Northway, M. J., DeCarlo, P. F., Kolb, C. E., Davidovits, P., and Worsnop, D. R.: Chemical and microphysical characterization of ambient aerosols with the aerodyne aerosol mass spectrometer, Mass Spectrom. Rev., 26, 185-222, https://doi.org/10.1002/mas.20115, 2007.

Capouet, M. and Müller, J. F.: A group contribution method for estimating the vapour pressures of α-pinene oxidation products, Atmos. Chem. Phys., 6, 1455-1467, https://doi.org/10.5194/acp-6-1455-2006, 2006.

Chen, W., Ye, Y. Q., Hu, W. W., Zhou, H. S., Pan, T. L., Wang, Y. K., Song, W., Song, Q. C., Ye, C. S., Wang, C. M., Wang, B. L., Huang, S., Yuan, B., Zhu, M., Lian, X. F., Zhang, G. H., Bi, X. H., Jiang, F., Liu, J. W., Canonaco, F., Prevot, A. S. H., Shao, M., and Wang, X. M.: Real-Time Characterization of Aerosol Compositions, Sources, and Aging Processes in

https://doi.org/10.5194/acp-2023-8
Preprint. Discussion started: 16 January 2023
© Author(s) 2023. CC BY 4.0 License.

Atmospheric Chemistry and Physics Discussions

Guangzhou During PRIDE-GBA 2018 Campaign, J. Geophys. Res.: Atmos., 126, e2021JD035114. , 10.1029/2021JD035114, 2021a.

Chen, X., Wang, H., and Lu, K.: Interpretation of NO3–N2O5 observation via steady state in high-aerosol air mass: the impact of equilibrium coefficient in ambient conditions, Atmos. Chem. Phys., 22, 3525-3533, 10.5194/acp-22-3525-2022, 2022.

Chen, Y., Zheng, P., Wang, Z., Pu, W., Tan, Y., Yu, C., Xia, M., Wang, W., Guo, J., Huang, D., Yan, C., Nie, W., Ling, Z., Chen, Q., Lee, S., and Wang, T.: Secondary Formation and Impacts of Gaseous Nitro-Phenolic Compounds in the Continental Outflow Observed at a Background Site in South China, Environ. Sci. Technol., 10.1021/acs.est.1c04596, 2021b.

Cheng, Y., Engling, G., He, K. B., Duan, F. K., Ma, Y. L., Du, Z. Y., Liu, J. M., Zheng, M., and Weber, R. J.: Biomass burning contribution to Beijing aerosol, Atmos. Chem. Phys., 13, 7765-7781, 10.5194/acp-13-7765-2013, 2013.

Coggon, M. M., Gkatzelis, G. I., McDonald, B. C., Gilman, J. B., Schwantes, R. H., Abuhassan, N., Aikin, K. C., Arend, M. F., Berkoff, T. A., Brown, S. S., Campos, T. L., Dickerson, R. R., Gronoff, G., Hurley, J. F., Isaacman-VanWertz, G., Koss, A. R., Li, M., McKeen, S. A., Moshary, F., Peischl, J., Pospisilova, V., Ren, X., Wilson, A., Wu, Y., Trainer, M., and Warneke, C.: Volatile chemical product emissions enhance ozone and modulate urban chemistry, Proc. Natl. Acad. Sci. U. S. A., 118, e2026653118, https://doi.org/10.1073/pnas.2026653118, 2021.

Cubison, M. J., Ortega, A. M., Hayes, P. L., Farmer, D. K., Day, D., Lechner, M. J., Brune, W. H., Apel, E., Diskin, G. S., Fisher, J. A., Fuelberg, H. E., Hecobian, A., Knapp, D. J., Mikoviny, T., Riemer, D., Sachse, G. W., Sessions, W., Weber, R. J., Weinheimer, A. J., Wisthaler, A., and Jimenez, J. L.: Effects of aging on organic aerosol from open biomass burning smoke in aircraft and laboratory studies, Atmos. Chem. Phys., 11, 12049-12064, https://doi.org/10.5194/acp-11-12049-2011, 2011.

Dancey, C. and Reidy, J.: Statistics without Maths for Psychology, London: Prentice Hall Paerson.2007.

Day, D. A., Liu, S., Russell, L. M., and Ziemann, P. J.: Organonitrate group concentrations in submicron particles with high nitrate and organic fractions in coastal southern California, Atmos. Environ., 44, 1970-1979, 10.1016/j.atmosenv.2010.02.045, 2010.

Day, D. A., Wooldridge, P. J., Dillon, M. B., Thornton, J. A., and Cohen, R. C.: A thermal dissociation laser-induced fluorescence instrument for in situ detection of NO2, peroxy nitrates, alkyl nitrates, and HNO3, Journal of Geophysical Research-Atmospheres, 107, ACH 4-1-ACH 4-14, 10.1029/2001jd000779, 2002.

Day, D. A., Campuzano-Jost, P., Nault, B. A., Palm, B. B., Hu, W., Guo, H., Wooldridge, P. J., Cohen, R. C., Docherty, K. S., Huffman, J. A., de Sá, S. S., Martin, S. T., and Jimenez, J. L.: A systematic re-evaluation of methods for quantification of bulk particle-phase organic nitrates using real-time aerosol mass spectrometry, Atmos. Meas. Tech., 15, 459-483, 10.5194/amt-15-459-2022, 2022.

DeCarlo, P. F., Kimmel, J. R., Trimborn, A., Northway, M. J., Jayne, J. T., Aiken, A. C., Gonin, M., Fuhrer, K., Horvath, T., Docherty, K. S., Worsnop, D. R., and Jimenez, J. L.: Field-Deployable, High-Resolution, Time-of-Flight Aerosol Mass Spectrometer, Anal. Chem., 78, 8281-8289, https://doi.org/10.1021/ac061249n, 2006.

Ditto, J. C., Machesky, J., and Gentner, D. R.: Analysis of reduced and oxidized nitrogen-containing organic compounds at a coastal site in summer and winter, Atmos. Chem. Phys., 22, 3045-3065, 10.5194/acp-22-3045-2022, 2022.

Farmer, D. K., Matsunaga, A., Docherty, K. S., Surratt, J. D., Seinfeld, J. H., Ziemann, P. J., and Jimenez, J. L.: Response of an aerosol mass spectrometer to organonitrates and organosulfates and implications for atmospheric chemistry, Proc. Natl. Acad. Sci. U. S. A., 107, 6670-6675, 10.1073/pnas.0912340107, 2010.

Farmer, D. K., Perring, A. E., Wooldridge, P. J., Blake, D. R., Baker, A., Meinardi, S., Huey, L. G., Tanner, D., Vargas, O., and Cohen, R. C.: Impact of organic nitrates on urban ozone production, Atmos. Chem. Phys., 11, 4085-4094, 10.5194/acp-11-4085-2011, 2011.

Faxon, C., Hammes, J., Le Breton, M., Pathak, R. K., and Hallquist, M.: Characterization of organic nitrate constituents of secondary organic aerosol (SOA) from nitrate-radical-initiated oxidation of limonene using high-resolution chemical ionization mass spectrometry, Atmos. Chem. Phys., 18, 5467-5481, 10.5194/acp-18-5467-2018, 2018.

Fisher, J. A., Jacob, D. J., Travis, K. R., Kim, P. S., Marais, E. A., Miller, C. C., Yu, K., Zhu, L., Yantosca, R. M., Sulprizio, M. P., Mao, J., Wennberg, P. O., Crounse, J. D., Teng, A. P., Nguyen, T. B., St Clair, J. M., Cohen, R. C., Romer, P., Nault, B. A., Wooldridge, P. J., Jimenez, J. L., Campuzano-Jost, P., Day, D. A., Hu, W., Shepson, P. B., Xiong, F., Blake, D. R., Goldstein, A. H., Misztal, P. K., Hanisco, T. F., Wolfe, G. M., Ryerson, T. B., Wisthaler, A., and Mikoviny, T.: Organic nitrate chemistry and its implications for nitrogen budgets in an isoprene- and monoterpene-rich atmosphere: constraints from aircraft (SEAC(4)RS) and ground-based (SOAS) observations in the Southeast US, Atmos. Chem. Phys., 16, 5969-5991, 10.5194/acp-16-5969-2016, 2016.

Fry, J. L., Draper, D. C., Zarzana, K. J., Campuzano-Jost, P., Day, D. A., Jimenez, J. L., Brown, S. S., Cohen, R. C., Kaser, L., Hansel, A., Cappellin, L., Karl, T., Roux, A. H., Turnipseed, A., Cantrell, C., Lefer, B. L., and Grossberg, N.: Observations of

https://doi.org/10.5194/acp-2023-8
Preprint. Discussion started: 16 January 2023
© Author(s) 2023. CC BY 4.0 License.

Atmospheric Chemistry and Physics Discussions

gas- and aerosol-phase organic nitrates at BEACHON-RoMBAS 2011, Atmos. Chem. Phys., 13, 8585-8605, 10.5194/acp-13-8585-2013, 2013.

Fry, J. L., Brown, S. S., Middlebrook, A. M., Edwards, P. M., Campuzano-Jost, P., Day, D. A., Jimenez, J. L., Allen, H. M., Ryerson, T. B., Pollack, I., Graus, M., Warneke, C., de Gouw, J. A., Brock, C. A., Gilman, J., Lerner, B. M., Dubé, W. P., Liao, J., and Welti, A.: Secondary organic aerosol (SOA) yields from NO3 radical + isoprene based on nighttime aircraft power plant plume transects, Atmos. Chem. Phys., 18, 11663-11682, 10.5194/acp-18-11663-2018, 2018.

Gaston, C. J., Lopez-Hilfiker, F. D., Whybrew, L. E., Hadley, O., McNair, F., Gao, H., Jaffe, D. A., and Thornton, J. A.: Online molecular characterization of fine particulate matter in Port Angeles, WA: Evidence for a major impact from residential wood smoke, Atmos. Environ., 138, 99-107, https://doi.org/10.1016/j.atmosenv.2016.05.013, 2016.

George, C., Ammann, M., D'Anna, B., Donaldson, D. J., and Nizkorodov, S. A.: Heterogeneous photochemistry in the atmosphere, Chem. Rev., 115, 4218-4258, https://doi.org/10.1021/cr500648z, 2015.

George, I. J. and Abbatt, J. P.: Heterogeneous oxidation of atmospheric aerosol particles by gas-phase radicals, Nature Chemistry, 2, 713-722, https://doi.org/10.1038/nchem.806, 2010.

Gkatzelis, G. I., Coggon, M. M., McDonald, B. C., Peischl, J., Aikin, K. C., Gilman, J. B., Trainer, M., and Warneke, C.: Identifying Volatile Chemical Product Tracer Compounds in U.S. Cities, Environ. Sci. Technol., 55, 188-199, https://doi.org/10.1021/acs.est.0c05467, 2021.

Gross, S., Iannone, R., Xiao, S., and Bertram, A. K.: Reactive uptake studies of NO3 and N2O5 on alkenoic acid, alkanoate, and polyalcohol substrates to probe nighttime aerosol chemistry, Phys. Chem. Chem. Phys., 11, 7792-7803, https://doi.org/10.1039/B904741G, 2009.

Hamilton, J. F., Bryant, D. J., Edwards, P. M., Ouyang, B., Bannan, T. J., Mehra, A., Mayhew, A. W., Hopkins, J. R., Dunmore, R. E., Squires, F. A., Lee, J. D., Newland, M. J., Worrall, S. D., Bacak, A., Coe, H., Percival, C., Whalley, L. K., Heard, D. E., Slater, E. J., Jones, R. L., Cui, T., Surratt, J. D., Reeves, C. E., Mills, G. P., Grimmond, S., Sun, Y., Xu, W., Shi, Z., and Rickard, A. R.: Key Role of NO3 Radicals in the Production of Isoprene Nitrates and Nitrooxyorganosulfates in Beijing, Environ. Sci. Technol., 55, 842-853, https://doi.org/10.1021/acs.est.0c05689, 2021.

Hao, L. Q., Kortelainen, A., Romakkaniemi, S., Portin, H., Jaatinen, A., Leskinen, A., Komppula, M., Miettinen, P., Sueper, D., Pajunoja, A., Smith, J. N., Lehtinen, K. E. J., Worsnop, D. R., Laaksonen, A., and Virtanen, A.: Atmospheric submicron aerosol composition and particulate organic nitrate formation in a boreal forestland–urban mixed region, Atmos. Chem. Phys., 14, 13483-13495, https://doi.org/10.5194/acp-14-13483-2014, 2014.

Harrison, R. M., Tilling, R., Callén Romero, M. a. S., Harrad, S., and Jarvis, K.: A study of trace metals and polycyclic aromatic hydrocarbons in the roadside environment, Atmos. Environ., 37, 2391-2402, https://doi.org/10.1016/S1352-2310(03)00122-5, 2003.

He, Q., Tomaz, S., Li, C., Zhu, M., Meidan, D., Riva, M., Laskin, A., Brown, S. S., George, C., Wang, X., and Rudich, Y.: Optical Properties of Secondary Organic Aerosol Produced by Nitrate Radical Oxidation of Biogenic Volatile Organic Compounds, Environ. Sci. Technol., 55, 2878-2889, https://doi.org/10.1021/acs.est.0c06838, 2021.

Hellén, H., Tykkä, T., and Hakola, H.: Importance of monoterpenes and isoprene in urban air in northern Europe, Atmos. Environ., 59, 59-66, https://doi.org/10.1016/j.atmosenv.2012.04.049, 2012.

Hennigan, C. J., Sullivan, A. P., Collett, J. L., and Robinson, A. L.: Levoglucosan stability in biomass burning particles exposed to hydroxyl radicals, Geophys. Res. Lett., 37, n/a-n/a, 10.1029/2010gl043088, 2010.

Hilas, C. S., Goudos, S. K., and Sahalos, J. N.: Seasonal decomposition and forecasting of telecommunication data: A comparative case study, Technological Forecasting and Social Change, 73, 495-509, https://doi.org/10.1016/j.techfore.2005.07.002, 2006.

Hoffmann, D., Tilgner, A., Iinuma, Y., and Herrmann, H.: Atmospheric Stability of Levoglucosan: A Detailed Laboratory and Modeling Study, Environ. Sci. Technol., 44, 694-699, 10.1021/es902476f, 2010.

Huang, W., Saathoff, H., Shen, X., Ramisetty, R., Leisner, T., and Mohr, C.: Chemical Characterization of Highly Functionalized Organonitrates Contributing to Night-Time Organic Aerosol Mass Loadings and Particle Growth, Environ. Sci. Technol., 53, 1165-1174, https://doi.org/10.1021/acs.est.8b05826, 2019.

Huffman, J. A., Ziemann, P. J., Jayne, J. T., Worsnop, D. R., and Jimenez, J. L.: Development and Characterization of a Fast-Stepping/Scanning Thermodenuder for Chemically-Resolved Aerosol Volatility Measurements, Aerosol Sci. Technol., 42, 395-407, https://doi.org/10.1080/02786820802104981, 2008.

Iyer, S., Rissanen, M. P., Valiev, R., Barua, S., Krechmer, J. E., Thornton, J., Ehn, M., and Kurtén, T.: Molecular mechanism for rapid autoxidation in α-pinene ozonolysis, Nat. Commun., 12, 878., https://doi.org/10.1038/s41467-021-21172-w, 2021.

© Author(s) 2023. CC BY 4.0 License.

Juncosa Calahorrano, J. F., Lindaas, J., O'Dell, K., Palm, B. B., Peng, Q., Flocke, F., Pollack, I. B., Garofalo, L. A., Farmer, D. K., Pierce, J. R., Collett Jr, J. L., Weinheimer, A., Campos, T., Hornbrook, R. S., Hall, S. R., Ullmann, K., Pothier, M. A., Apel, E. C., Permar, W., Hu, L., Hills, A. J., Montzka, D., Tyndall, G., Thornton, J. A., and Fischer, E. V.: Daytime Oxidized Reactive Nitrogen Partitioning in Western U.S. Wildfire Smoke Plumes, J. Geophys. Res.: Atmos., 126, e2020JD033484, https://doi.org/10.1029/2020JD033484, 2021.

Keehan, N. I., Brownwood, B., Marsavin, A., Day, D. A., and Fry, J. L.: A thermal-dissociation–cavity ring-down spectrometer (TD-CRDS) for the detection of organic nitrates in gas and particle phases, Atmos. Meas. Tech., 13, 6255-6269, https://doi.org/10.5194/amt-13-6255-2020, 2020.

Kiendler-Scharr, A., Mensah, A. A., Friese, E., Topping, D., Nemitz, E., Prevot, A. S. H., Äijälä, M., Allan, J., Canonaco, F., Canagaratna, M., Carbone, S., Crippa, M., Dall Osto, M., Day, D. A., De Carlo, P., Di Marco, C. F., Elbern, H., Eriksson, A., Freney, E., Hao, L., Herrmann, H., Hildebrandt, L., Hillamo, R., Jimenez, J. L., Laaksonen, A., McFiggans, G., Mohr, C., O'Dowd, C., Otjes, R., Ovadnevaite, J., Pandis, S. N., Poulain, L., Schlag, P., Sellegri, K., Swietlicki, E., Tiitta, P., Vermeulen, A., Wahner, A., Worsnop, D., and Wu, H. C.: Ubiquity of organic nitrates from nighttime chemistry in the European submicron aerosol, Geophys. Res. Lett., 43, 7735-7744, https://doi.org/10.1002/2016gl069239, 2016.

Koch, B. P. and Dittmar, T.: From mass to structure: an aromaticity index for high-resolution mass data of natural organic matter, Rapid Commun. Mass Spectrom., 20, 926-932, https://doi.org/10.1002/rcm.2386, 2006.

Koch, B. P. and Dittmar, T.: From mass to structure: an aromaticity index for high-resolution mass data of natural organic matter, Rapid Commun. Mass Spectrom., 30, 250-250, https://doi.org/10.1002/rcm.7433, 2016.

Kodros, J. K., Papanastasiou, D. K., Paglione, M., Masiol, M., Squizzato, S., Florou, K., Skyllakou, K., Kaltsonoudis, C., Nenes, A., and Pandis, S. N.: Rapid dark aging of biomass burning as an overlooked source of oxidized organic aerosol, Proc. Natl. Acad. Sci. U. S. A., 117, 33028-33033, https://doi.org/10.1073/pnas.2010365117, 2020.

Krecl, P., Johansson, C., Targino, A. C., Ström, J., and Burman, L.: Trends in black carbon and size-resolved particle number concentrations and vehicle emission factors under real-world conditions, Atmos. Environ., 165, 155-168, https://doi.org/10.1016/j.atmosenv.2017.06.036, 2017.

Kroll, J. H. and Seinfeld, J. H.: Chemistry of secondary organic aerosol: Formation and evolution of low-volatility organics in the atmosphere, Atmos. Environ., 42, 3593-3624, https://doi.org/10.1016/j.atmosenv.2008.01.003, 2008.

Lai, C., Liu, Y., Ma, J., Ma, Q., and He, H.: Degradation kinetics of levoglucosan initiated by hydroxyl radical under different environmental conditions, Atmos. Environ., 91, 32-39, https://doi.org/10.1016/j.atmosenv.2014.03.054, 2014.

Lanz, V. A., Prévôt, A. S. H., Alfarra, M. R., Weimer, S., Mohr, C., DeCarlo, P. F., Gianini, M. F. D., Hueglin, C., Schneider, J., Favez, O., D'Anna, B., George, C., and Baltensperger, U.: Characterization of aerosol chemical composition with aerosol mass spectrometry in Central Europe: an overview, Atmos. Chem. Phys., 10, 10453-10471, https://doi.org/10.5194/acp-10-10453-2010, 2010.

Le Breton, M., Psichoudaki, M., Hallquist, M., Watne, Å. K., Lutz, A., and Hallquist, Å. M.: Application of a FIGAERO ToF CIMS for on-line characterization of real-world fresh and aged particle emissions from buses, Aerosol Sci. Technol., 53, 244-259, https://doi.org/10.1080/02786826.2019.1566592, 2019.

Lee, A. K. Y., Adam, M. G., Liggio, J., Li, S.-M., Li, K., Willis, M. D., Abbatt, J. P. D., Tokarek, T. W., Odame-Ankrah, C. A., Osthoff, H. D., Strawbridge, K., and Brook, J. R.: A large contribution of anthropogenic organo-nitrates to secondary organic aerosol in the Alberta oil sands, Atmos. Chem. Phys., 19, 12209-12219, https://doi.org/10.5194/acp-19-12209-2019, 2019.

Lee, B. H., Lopez-Hilfiker, F. D., Mohr, C., Kurten, T., Worsnop, D. R., and Thornton, J. A.: An iodide-adduct high-resolution time-of-flight chemical-ionization mass spectrometer: application to atmospheric inorganic and organic compounds, Environ. Sci. Technol., 48, 6309-6317, https://doi.org/10.1021/es500362a, 2014.

Lee, B. H., Lopez-Hilfiker, F. D., D'Ambro, E. L., Zhou, P., Boy, M., Petäjä, T., Hao, L., Virtanen, A., and Thornton, J. A.: Semi-volatile and highly oxygenated gaseous and particulate organic compounds observed above a boreal forest canopy, Atmos. Chem. Phys., 18, 11547-11562, https://doi.org/10.5194/acp-18-11547-2018, 2018.

Lee, B. H., Mohr, C., Lopez-Hilfiker, F. D., Lutz, A., Hallquist, M., Lee, L., Romer, P., Cohen, R. C., Iyer, S., Kurten, T., Hu, W., Day, D. A., Campuzano-Jost, P., Jimenez, J. L., Xu, L., Ng, N. L., Guo, H., Weber, R. J., Wild, R. J., Brown, S. S., Koss, A., de Gouw, J., Olson, K., Goldstein, A. H., Seco, R., Kim, S., McAvey, K., Shepson, P. B., Starn, T., Baumann, K., Edgerton, E. S., Liu, J., Shilling, J. E., Miller, D. O., Brune, W., Schobesberger, S., D'Ambro, E. L., and Thornton, J. A.: Highly functionalized organic nitrates in the southeast United States: Contribution to secondary organic aerosol and reactive nitrogen budgets, Proc. Natl. Acad. Sci. U. S. A., 113, 1516-1521, https://doi.org/10.1073/pnas.1508108113, 2016.

Lee, C. P., Surdu, M., Bell, D. M., Lamkaddam, H., Wang, M., Ataei, F., Hofbauer, V., Lopez, B., Donahue, N. M., Dommen, J., Prevot, A. S. H., Slowik, J. G., Wang, D., Baltensperger, U., and El Haddad, I.: Effects of aerosol size and coating thickness

https://doi.org/10.5194/acp-2023-8
Preprint. Discussion started: 16 January 2023
© Author(s) 2023. CC BY 4.0 License.

Atmospheric Chemistry and Physics Discussions

on the molecular detection using extractive electrospray ionization, Atmos. Meas. Tech., 14, 5913-5923, 10.5194/amt-14-5913-2021, 2021.

Lee, L., Wooldridge, P. J., deGouw, J., Brown, S. S., Bates, T. S., Quinn, P. K., and Cohen, R. C.: Particulate organic nitrates observed in an oil and natural gas production region during wintertime, Atmos. Chem. Phys., 15, 9313-9325, https://doi.org/10.5194/acp-15-9313-2015, 2015.

Li, T., Wang, Z., Yuan, B., Ye, C., Lin, Y., Wang, S., Sha, Q. e., Yuan, Z., Zheng, J., and Shao, M.: Emissions of carboxylic acids, hydrogen cyanide (HCN) and isocyanic acid (HNCO) from vehicle exhaust, Atmos. Environ., 247, 118218., https://doi.org/10.1016/j.atmosenv.2021.118218, 2021a.

Li, X. B., Yuan, B., Wang, S., Wang, C., Lan, J., Liu, Z., Song, Y., He, X., Huangfu, Y., Pei, C., Cheng, P., Yang, S., Qi, J., Wu, C., Huang, S., You, Y., Chang, M., Zheng, H., Yang, W., Wang, X., and Shao, M.: Variations and sources of volatile organic compounds (VOCs) in urban region: insights from measurements on a tall tower, Atmos. Chem. Phys., 22, 10567-10587, 10.5194/acp-22-10567-2022, 2022.

Li, Y., Fu, T. M., Yu, J. Z., Feng, X., Zhang, L., Chen, J., Boreddy, S. K. R., Kawamura, K., Fu, P., Yang, X., Zhu, L., and Zeng, Z.: Impacts of Chemical Degradation on the Global Budget of Atmospheric Levoglucosan and Its Use As a Biomass Burning Tracer, Environ. Sci. Technol., 55, 5525-5536, https://doi.org/10.1021/acs.est.0c07313, 2021b.

Liebmann, J., Sobanski, N., Schuladen, J., Karu, E., Hellén, H., Hakola, H., Zha, Q., Ehn, M., Riva, M., Heikkinen, L., Williams, J., Fischer, H., Lelieveld, J., and Crowley, J. N.: Alkyl nitrates in the boreal forest: formation via the NO3-, OH- and O3 induced oxidation of biogenic volatile organic compounds and ambient lifetimes, Atmos. Chem. Phys., 19, 10391-10403, https://doi.org/10.5194/acp-19-10391-2019, 2019.

Lim, Y. B. and Ziemann, P. J.: Chemistry of Secondary Organic Aerosol Formation from OH Radical-Initiated Reactions of Linear, Branched, and Cyclic Alkanes in the Presence of NOx, Aerosol Sci. Technol., 43, 604-619, https://doi.org/10.1080/02786820902802567, 2009.

Lin, P., Bluvshtein, N., Rudich, Y., Nizkorodov, S. A., Laskin, J., and Laskin, A.: Molecular Chemistry of Atmospheric Brown Carbon Inferred from a Nationwide Biomass Burning Event, Environ. Sci. Technol., 51, 11561-11570, https://doi.org/10.1021/acs.est.7b02276, 2017.

Liu, X., Huey, L. G., Yokelson, R. J., Selimovic, V., Simpson, I. J., Müller, M., Jimenez, J. L., Campuzano-Jost, P., Beyersdorf, A. J., Blake, D. R., Butterfield, Z., Choi, Y., Crounse, J. D., Day, D. A., Diskin, G. S., Dubey, M. K., Fortner, E., Hanisco, T. F., Hu, W., King, L. E., Kleinman, L., Meinardi, S., Mikoviny, T., Onasch, T. B., Palm, B. B., Peischl, J., Pollack, I. B., Ryerson, T. B., Sachse, G. W., Sedlacek, A. J., Shilling, J. E., Springston, S., St. Clair, J. M., Tanner, D. J., Teng, A. P., Wennberg, P. O., Wisthaler, A., and Wolfe, G. M.: Airborne measurements of western U.S. wildfire emissions: Comparison with prescribed burning and air quality implications, J. Geophys. Res.: Atmos., 122, 6108-6129, https://doi.org/10.1002/2016jd026315, 2017.

Lopez-Hilfiker, F., Mohr, C., Ehn, M., Rubach, F., Kleist, E., Wildt, J., Mentel, T., Lutz, A., Hallquist, M., Worsnop, D., and Thornton, J.: A novel method for online analysis of gas and particle composition: description and evaluation of a Filter Inlet for Gases and AEROsols (FIGAERO), Atmos. Meas. Tech., 7, 983–1001, https://doi.org/10.5194/amt-7-983-2014, 2014.

Lopez-Hilfiker, F. D., Pospisilova, V., Huang, W., Kalberer, M., Mohr, C., Stefenelli, G., Thornton, J. A., Baltensperger, U., Prevot, A. S. H., and Slowik, J. G.: An extractive electrospray ionization time-of-flight mass spectrometer (EESI-TOF) for online measurement of atmospheric aerosol particles, Atmos. Meas. Tech., 12, 4867-4886, https://doi.org/10.5194/amt-12-4867-2019, 2019.

Lopez-Hilfiker, F. D., Mohr, C., D'Ambro, E. L., Lutz, A., Riedel, T. P., Gaston, C. J., Iyer, S., Zhang, Z., Gold, A., Surratt, J. D., Lee, B. H., Kurten, T., Hu, W. W., Jimenez, J., Hallquist, M., and Thornton, J. A.: Molecular Composition and Volatility of Organic Aerosol in the Southeastern U.S.: Implications for IEPOX Derived SOA, Environ. Sci. Technol., 50, 2200-2209, https://doi.org/10.1021/acs.est.5b04769, 2016.

Matsunaga, A. and Ziemann, P. J.: Yields of beta-hydroxynitrates, dihydroxynitrates, and trihydroxynitrates formed from OH radical-initiated reactions of 2-methyl-1-alkenes, Proc. Natl. Acad. Sci. U. S. A., 107, 6664-6669, https://doi.org/10.1073/pnas.0910585107, 2010.

Mayhew, A. W., Lee, B. H., Thornton, J. A., Bannan, T. J., Brean, J., Hopkins, J. R., Lee, J. D., Nelson, B. S., Percival, C., Rickard, A. R., Shaw, M. D., Edwards, P. M., and Hamilton, J. F.: Evaluation of isoprene nitrate chemistry in detailed chemical mechanisms, Atmos. Chem. Phys., 22, 14783-14798, 10.5194/acp-22-14783-2022, 2022.

Mayorga, R., Xia, Y., Zhao, Z., Long, B., and Zhang, H.: Peroxy Radical Autoxidation and Sequential Oxidation in Organic Nitrate Formation during Limonene Nighttime Oxidation, Environ. Sci. Technol., 10.1021/acs.est.2c04030, 2022.

McKay, M. D., Beckman, R. J., and Conover, W. J.: A Comparison of Three Methods for Selecting Values of Input Variables in the Analysis of Output From a Computer Code, Technometrics, 42, 55-61, 10.1080/00401706.2000.10485979, 2000.

https://doi.org/10.5194/acp-2023-8
Preprint. Discussion started: 16 January 2023
© Author(s) 2023. CC BY 4.0 License.

Atmospheric Chemistry and Physics Discussions

Mohr, C., Huffman, J. A., Cubison, M. J., Aiken, A. C., Docherty, K. S., Kimmel, J. R., Ulbrich, I. M., Hannigan, M., and Jimenez, J. L.: Characterization of Primary Organic Aerosol Emissions from Meat Cooking, Trash Burning, and Motor Vehicles with High-Resolution Aerosol Mass Spectrometry and Comparison with Ambient and Chamber Observations, Environ. Sci. Technol., 43, 2443-2449, 10.1021/es8011518, 2009.

Mohr, C., Lopez-Hilfiker, F. D., Zotter, P., Prévôt, A. S. H., Xu, L., Ng, N. L., Herndon, S. C., Williams, L. R., Franklin, J. P., Zahniser, M. S., Worsnop, D. R., Knighton, W. B., Aiken, A. C., Gorkowski, K. J., Dubey, M. K., Allan, J. D., and Thornton, J. A.: Contribution of Nitrated Phenols to Wood Burning Brown Carbon Light Absorption in Detling, United Kingdom during Winter Time, Environ. Sci. Technol., 47, 6316-6324, https://doi.org/10.1021/es400683v, 2013.

Ng, N. L., Brown, S. S., Archibald, A. T., Atlas, E., Cohen, R. C., Crowley, J. N., Day, D. A., Donahue, N. M., Fry, J. L., Fuchs, H., Griffin, R. J., Guzman, M. I., Herrmann, H., Hodzic, A., Iinuma, Y., Jimenez, J. L., Kiendler-Scharr, A., Lee, B. H., Luecken, D. J., Mao, J., McLaren, R., Mutzel, A., Osthoff, H. D., Ouyang, B., Picquet-Varrault, B., Platt, U., Pye, H. O. T., Rudich, Y., Schwantes, R. H., Shiraiwa, M., Stutz, J., Thornton, J. A., Tilgner, A., Williams, B. J., and Zaveri, R. A.: Nitrate radicals and biogenic volatile organic compounds: oxidation, mechanisms, and organic aerosol, Atmos. Chem. Phys., 17, 2103-2162, https://doi.org/10.5194/acp-17-2103-2017, 2017.

Odum, J. R., Hoffmann, T., Bowman, F., Collins, D., Flagan, R. C., and Seinfeld, J. H.: Gas/Particle Partitioning and Secondary Organic Aerosol Yields, Environ. Sci. Technol., 30, 2580-2585, https://doi.org/10.1021/es950943+, 1996.

Palm, B. B., Liu, X., Jimenez, J. L., and Thornton, J. A.: Performance of a new coaxial ion–molecule reaction region for low-pressure chemical ionization mass spectrometry with reduced instrument wall interactions, Atmos. Meas. Tech., 12, 5829-5844, 10.5194/amt-12-5829-2019, 2019.

Palm, B. B., Peng, Q., Fredrickson, C. D., Lee, B. H., Garofalo, L. A., Pothier, M. A., Kreidenweis, S. M., Farmer, D. K., Pokhrel, R. P., Shen, Y., Murphy, S. M., Permar, W., Hu, L., Campos, T. L., Hall, S. R., Ullmann, K., Zhang, X., Flocke, F., Fischer, E. V., and Thornton, J. A.: Quantification of organic aerosol and brown carbon evolution in fresh wildfire plumes, Proc. Natl. Acad. Sci. U. S. A., 117, 29469-29477, https://doi.org/10.1073/pnas.2012218117, 2020.

Peng, Q., Palm, B. B., Fredrickson, C. D., Lee, B. H., Hall, S. R., Ullmann, K., Campos, T., Weinheimer, A. J., Apel, E. C., Flocke, F., Permar, W., Hu, L., Garofalo, L. A., Pothier, M. A., Farmer, D. K., Ku, I. T., Sullivan, A. P., Collett, J. L., Fischer, E., and Thornton, J. A.: Observations and Modeling of NOx Photochemistry and Fate in Fresh Wildfire Plumes, ACS Earth Space Chem., 10.1021/acsearthspacechem.1c00086, 2021.

Perring, A. E., Pusede, S. E., and Cohen, R. C.: An observational perspective on the atmospheric impacts of alkyl and multifunctional nitrates on ozone and secondary organic aerosol, Chem. Rev., 113, 5848-5870, https://doi.org/10.1021/cr300520x, 2013.

Pospisilova, V., Lopez-Hilfiker., F. D., Bell., D. M., Haddad., I. E., Mohr., C., Huang., W., Heikkinen., L., Xiao., M., Dommen., J., Prevot., A. S. H., Baltensperger., U., and Slowik., J. G.: On the fate of oxygenated organic molecules in atmospheric aerosol particles, Sci. Adv., 6, eaax8922, https://doi.org/10.1126/sciadv.aax8922, 2020.

Pye, H. O., Luecken, D. J., Xu, L., Boyd, C. M., Ng, N. L., Baker, K. R., Ayres, B. R., Bash, J. O., Baumann, K., Carter, W. P., Edgerton, E., Fry, J. L., Hutzell, W. T., Schwede, D. B., and Shepson, P. B.: Modeling the Current and Future Roles of Particulate Organic Nitrates in the Southeastern United States, Environ. Sci. Technol., 49, 14195-14203, https://doi.org/10.1021/acs.est.5b03738, 2015.

Pye, H. O. T., D'Ambro, E. L., Lee, B. H., Schobesberger, S., Takeuchi, M., Zhao, Y., Lopez-Hilfiker, F., Liu, J., Shilling, J. E., Xing, J., Mathur, R., Middlebrook, A. M., Liao, J., Welti, A., Graus, M., Warneke, C., de Gouw, J. A., Holloway, J. S., Ryerson, T. B., Pollack, I. B., and Thornton, J. A.: Anthropogenic enhancements to production of highly oxygenated molecules from autoxidation, Proc. Natl. Acad. Sci. U. S. A., 116, 6641-6646, https://doi.org/10.1073/pnas.1810774116, 2019.

Reeves, C. E., Mills, G. P., Whalley, L. K., Acton, W. J. F., Bloss, W. J., Crilley, L. R., Grimmond, S., Heard, D. E., Hewitt, C. N., Hopkins, J. R., Kotthaus, S., Kramer, L. J., Jones, R. L., Lee, J. D., Liu, Y., Ouyang, B., Slater, E., Squires, F., Wang, X., Woodward-Massey, R., and Ye, C.: Observations of speciated isoprene nitrates in Beijing: implications for isoprene chemistry, Atmos. Chem. Phys. Discuss., Preprint, 10.5194/acp-2019-964, 2020.

Rollins, A. W., Smith, J. D., Wilson, K. R., and Cohen, R. C.: Real Time In Situ Detection of Organic Nitrates in Atmospheric Aerosols, Environ. Sci. Technol., 44, 5540-5545, https://doi.org/10.1021/es100926x, 2010.

Rollins, A. W., Browne, E. C., Min, K. E., Pusede, S. E., Wooldridge, P. J., Gentner, D. R., Goldstein, A. H., Liu, S., Day, D. A., Russell, L. M., and Cohen, R. C.: Evidence for NO(x) control over nighttime SOA formation, Science, 337, 1210-1212, https://doi.org/10.1126/science.1221520, 2012.

Romer Present, P. S., Zare, A., and Cohen, R. C.: The changing role of organic nitrates in the removal and transport of NOx, Atmos. Chem. Phys., 20, 267-279, https://doi.org/10.5194/acp-20-267-2020, 2020.

https://doi.org/10.5194/acp-2023-8
Preprint. Discussion started: 16 January 2023
© Author(s) 2023. CC BY 4.0 License.

Romer, P. S., Duffey, K. C., Wooldridge, P. J., Allen, H. M., Ayres, B. R., Brown, S. S., Brune, W. H., Crounse, J. D., de Gouw, J., Draper, D. C., Feiner, P. A., Fry, J. L., Goldstein, A. H., Koss, A., Misztal, P. K., Nguyen, T. B., Olson, K., Teng, A. P., Wennberg, P. O., Wild, R. J., Zhang, L., and Cohen, R. C.: The lifetime of nitrogen oxides in an isoprene-dominated forest, Atmos. Chem. Phys., 16, 7623-7637, https://doi.org/10.5194/acp-16-7623-2016, 2016.

Sadanaga, Y., Takaji, R., Ishiyama, A., Nakajima, K., Matsuki, A., and Bandow, H.: Thermal dissociation cavity attenuated phase shift spectroscopy for continuous measurement of total peroxy and organic nitrates in the clean atmosphere, Review of Scientific Instruments, 87, 074102., https://doi.org/10.1063/1.4958167, 2016.

Salvador, C. M., Chou, C. C. K., Cheung, H. C., Ho, T. T., Tsai, C. Y., Tsao, T. M., Tsai, M. J., and Su, T. C.: Measurements of submicron organonitrate particles: Implications for the impacts of NOx pollution in a subtropical forest, Atmospheric Research, 245, https://doi.org/10.1016/j.atmosres.2020.105080, 2020.

Salvador, C. M. G., Tang, R., Priestley, M., Li, L., Tsiligiannis, E., Le Breton, M., Zhu, W., Zeng, L., Wang, H., Yu, Y., Hu, M., Guo, S., and Hallquist, M.: Ambient nitro-aromatic compounds – biomass burning versus secondary formation in rural China, Atmos. Chem. Phys., 21, 1389-1406, 10.5194/acp-21-1389-2021, 2021.

Sato, K., Takami, A., Isozaki, T., Hikida, T., Shimono, A., and Imamura, T.: Mass spectrometric study of secondary organic aerosol formed from the photo-oxidation of aromatic hydrocarbons, Atmos. Environ., 44, 1080-1087, https://doi.org/10.1016/j.atmosenv.2009.12.013, 2010.

Schobesberger, S., D'Ambro, E. L., Lopez-Hilfiker, F. D., Mohr, C., and Thornton, J. A.: A model framework to retrieve thermodynamic and kinetic properties of organic aerosol from composition-resolved thermal desorption measurements, Atmos. Chem. Phys., 18, 14757-14785, 10.5194/acp-18-14757-2018, 2018.

Shen, H., Zhao, D., Pullinen, I., Kang, S., Vereecken, L., Fuchs, H., Acir, I. H., Tillmann, R., Rohrer, F., Wildt, J., Kiendler-Scharr, A., Wahner, A., and Mentel, T. F.: Highly Oxygenated Organic Nitrates Formed from NO3 Radical-Initiated Oxidation of beta-Pinene, Environ. Sci. Technol., 10.1021/acs.est.1c03978, 2021.

Simoneit, B. R. T.: Biomass burning — a review of organic tracers for smoke from incomplete combustion, Appl. Geochem, 17, 129-162, https://doi.org/10.1016/S0883-2927(01)00061-0, 2002.

Simoneit, B. R. T., Schauer, J. J., Nolte, C. G., Oros, D. R., Elias, V. O., Fraser, M. P., Rogge, W. F., and Cass, G. R.: Levoglucosan, a tracer for cellulose in biomass burning and atmospheric particles, Atmos. Environ., 33, 173-182, https://doi.org/10.1016/S1352-2310(98)00145-9, 1999.

Singla, V., Mukherjee, S., Pandithurai, G., Dani, K. K., and Safai, P. D.: Evidence of Organonitrate Formation at a High Altitude Site, Mahabaleshwar, during the Pre-monsoon Season, Aerosol and Air Quality Research, 19, 1241-1251, https://doi.org/10.4209/aaqr.2018.03.0110, 2019.

Sobanski, N., Thieser, J., Schuladen, J., Sauvage, C., Song, W., Williams, J., Lelieveld, J., and Crowley, J. N.: Day and night-time formation of organic nitrates at a forested mountain site in south-west Germany, Atmos. Chem. Phys., 17, 4115-4130, https://doi.org/10.5194/acp-17-4115-2017, 2017.

Sommers, J. M., Stroud, C. A., Adam, M. G., O'Brien, J., Brook, J. R., Hayden, K., Lee, A. K. Y., Li, K., Liggio, J., Mihele, C., Mittermeier, R. L., Stevens, R. G., Wolde, M., Zuend, A., and Hayes, P. L.: Evaluating SOA formation from different sources of semi- and intermediate-volatility organic compounds from the Athabasca oil sands, Environmental Science: Atmospheres, 2, 469-490, 10.1039/D1EA00053E, 2022.

Song, K., Guo, S., Wang, H., Yu, Y., Wang, H., Tang, R., Xia, S., Gong, Y., Wan, Z., Lv, D., Tan, R., Zhu, W., Shen, R., Li, X., Yu, X., Chen, S., Zeng, L., and Huang, X.: Measurement Report: Online Measurement of Gas-Phase Nitrated Phenols Utilizing CI-LToF-MS: Primary Sources and Secondary Formation, Atmos. Chem. Phys., 21, 7917–7932, https://doi.org/10.5194/acp-2020-1294, 2021.

Sun, Y. L., Zhang, Q., Schwab, J. J., Yang, T., Ng, N. L., and Demerjian, K. L.: Factor analysis of combined organic and inorganic aerosol mass spectra from high resolution aerosol mass spectrometer measurements, Atmos. Chem. Phys., 12, 8537-8551, https://doi.org/10.5194/acp-12-8537-2012, 2012.

Takeuchi, M. and Ng, N. L.: Chemical composition and hydrolysis of organic nitrate aerosol formed from hydroxyl and nitrate radical oxidation of α-pinene and β-pinene, Atmos. Chem. Phys., 19, 12749-12766, https://doi.org/10.5194/acp-19-12749-2019, 2019.

Thornton, J. A., Mohr, C., Schobesberger, S., D'Ambro, E. L., Lee, B. H., and Lopez-Hilfiker, F. D.: Evaluating Organic Aerosol Sources and Evolution with a Combined Molecular Composition and Volatility Framework Using the Filter Inlet for Gases and Aerosols (FIGAERO), Acc Chem Res, 53, 1415-1426, 10.1021/acs.accounts.0c00259, 2020.

https://doi.org/10.5194/acp-2023-8
Preprint. Discussion started: 16 January 2023
© Author(s) 2023. CC BY 4.0 License.

Atmospheric Chemistry and Physics Discussions

Turpin, B. J. and Huntzicker, J. J.: Identification of secondary organic aerosol episodes and quantitation of primary and secondary organic aerosol concentrations during SCAQS, Atmos. Environ., 29, 3527-3544, https://doi.org/10.1016/1352-2310(94)00276-Q, 1995.

Urban, R. C., Lima-Souza, M., Caetano-Silva, L., Queiroz, M. E. C., Nogueira, R. F. P., Allen, A. G., Cardoso, A. A., Held, G., and Campos, M. L. A. M.: Use of levoglucosan, potassium, and water-soluble organic carbon to characterize the origins of biomass-burning aerosols, Atmos. Environ., 61, 562-569, https://doi.org/10.1016/j.atmosenv.2012.07.082, 2012.

Wang, C., Yuan, B., Wu, C., Wang, S., Qi, J., Wang, B., Wang, Z., Hu, W., Chen, W., Ye, C., Wang, W., Sun, Y., Wang, C., Huang, S., Song, W., Wang, X., Yang, S., Zhang, S., Xu, W., Ma, N., Zhang, Z., Jiang, B., Su, H., Cheng, Y., Wang, X., and Shao, M.: Measurements of higher alkanes using NO+ chemical ionization in PTR-ToF-MS: important contributions of higher alkanes to secondary organic aerosols in China, Atmos. Chem. Phys., 20, 14123-14138, https://doi.org/10.5194/acp-20-14123-2020, 2020a.

Wang, H., Lu, K., Chen, X., Zhu, Q., Chen, Q., Guo, S., Jiang, M., Li, X., Shang, D., Tan, Z., Wu, Y., Wu, Z., Zou, Q., Zheng, Y., Zeng, L., Zhu, T., Hu, M., and Zhang, Y.: High N2O5 Concentrations Observed in Urban Beijing: Implications of a Large Nitrate Formation Pathway, Environmental Science & Technology Letters, 4, 416-420, https://doi.org/10.1021/acs.estlett.7b00341, 2017a.

Wang, L., Wang, X., Gu, R., Wang, H., Yao, L., Wen, L., Zhu, F., Wang, W., Xue, L., Yang, L., Lu, K., Chen, J., Wang, T., Zhang, Y., and Wang, W.: Observations of fine particulate nitrated phenols in four sites in northern China: concentrations, source apportionment, and secondary formation, Atmos. Chem. Phys., 18, 4349-4359, https://doi.org/10.5194/acp-18-4349-2018, 2018.

Wang L.J, Wu D.L, and Zhang Z.S: Characterization of typical biomass burning tracers among atmospheric particles in urban Guangzhou, J. Grad. Univ. Chin. Acad. Sci., 34, 567-572, https://doi.org/10.7523/j.issn.2095-6134.2017.05.006, 2017.

Wang, M., Chen, D., Xiao, M., Ye, Q., Stolzenburg, D., Hofbauer, V., Ye, P., Vogel, A. L., Mauldin, R. L., 3rd, Amorim, A., Baccarini, A., Baumgartner, B., Brilke, S., Dada, L., Dias, A., Duplissy, J., Finkenzeller, H., Garmash, O., He, X. C., Hoyle, C. R., Kim, C., Kvashnin, A., Lehtipalo, K., Fischer, L., Molteni, U., Petaja, T., Pospisilova, V., Quelever, L. L. J., Rissanen, M., Simon, M., Tauber, C., Tome, A., Wagner, A. C., Weitz, L., Volkamer, R., Winkler, P. M., Kirkby, J., Worsnop, D. R., Kulmala, M., Baltensperger, U., Dommen, J., El-Haddad, I., and Donahue, N. M.: Photo-oxidation of Aromatic Hydrocarbons Produces Low-Volatility Organic Compounds, Environ. Sci. Technol., 54, 7911-7921, https://doi.org/10.1021/acs.est.0c02100, 2020b.

Wang, S. and Li, H.: NO3·-Initiated Gas-Phase Formation of Nitrated Phenolic Compounds in Polluted Atmosphere, Environ. Sci. Technol., 55, 2899-2907, https://doi.org/10.1021/acs.est.0c08041, 2021.

Wang, S., Peng, Y., Peng, Q., Wu, C., Wang, C., Wang, B., Wang, Z., Kuang, Y., Song, W., Wang, X., Hu, W., Chen, W., Shen, J., Chen, D., Shao, M., and Yuan, B.: Different chemical removal pathways of volatile organic compounds (VOCs): Comparison of urban and regional sites, Acta Sci. Circumstantiae, 40, 2311-2322, https://doi.org/10.13671/j.hjkxxb.2020.0153, 2020c.

Wang, S. H., Yuan, B., Wu, C. H., Wang, C. M., Li, T. G., He, X. J., Huangfu, Y. B., Qi, J. P., Li, X. B., Sha, Q. E., Zhu, M. N., Lou, S. R., Wang, H. L., Karl, T., Graus, M., Yuan, Z. B., and Shao, M.: Oxygenated volatile organic compounds (VOCs) as significant but varied contributors to VOC emissions from vehicles, Atmos. Chem. Phys., 22, 9703-9720, 10.5194/acp-22-9703-2022, 2022a.

Wang, Y., Hu, M., Lin, P., Guo, Q., Wu, Z., Li, M., Zeng, L., Song, Y., Zeng, L., Wu, Y., Guo, S., Huang, X., and He, L.: Molecular Characterization of Nitrogen-Containing Organic Compounds in Humic-like Substances Emitted from Straw Residue Burning, Environ. Sci. Technol., 51, 5951-5961, https://doi.org/10.1021/acs.est.7b00248, 2017b.

Wang, Y., Hu, M., Lin, P., Tan, T., Li, M., Xu, N., Zheng, J., Du, Z., Qin, Y., Wu, Y., Lu, S., Song, Y., Wu, Z., Guo, S., Zeng, L., Huang, X., and He, L.: Enhancement in Particulate Organic Nitrogen and Light Absorption of Humic-Like Substances over Tibetan Plateau Due to Long-Range Transported Biomass Burning Emissions, Environ. Sci. Technol., 53, 14222-14232, https://doi.org/10.1021/acs.est.9b06152, 2019.

Wang, Z., Shi, Z., Wang, F., Liang, W., Shi, G., Wang, W., Chen, D., Liang, D., Feng, Y., and Russell, A. G.: Implications for ozone control by understanding the survivor bias in observed ozone-volatile organic compounds system, npj Climate and Atmospheric Science, 5, 10.1038/s41612-022-00261-7, 2022b.

Wang, Z., Yuan, B., Ye, C., Roberts, J., Wisthaler, A., Lin, Y., Li, T., Wu, C., Peng, Y., Wang, C., Wang, S., Yang, S., Wang, B., Qi, J., Wang, C., Song, W., Hu, W., Wang, X., Xu, W., Ma, N., Kuang, Y., Tao, J., Zhang, Z., Su, H., Cheng, Y., Wang, X., and Shao, M.: High Concentrations of Atmospheric Isocyanic Acid (HNCO) Produced from Secondary Sources in China, Environ. Sci. Technol., 54, 11818-11826, https://doi.org/10.1021/acs.est.0c02843, 2020d.

https://doi.org/10.5194/acp-2023-8
Preprint. Discussion started: 16 January 2023
© Author(s) 2023. CC BY 4.0 License.

Wennberg, P. O., Bates, K. H., Crounse, J. D., Dodson, L. G., McVay, R. C., Mertens, L. A., Nguyen, T. B., Praske, E., Schwantes, R. H., Smarte, M. D., St Clair, J. M., Teng, A. P., Zhang, X., and Seinfeld, J. H.: Gas-Phase Reactions of Isoprene and Its Major Oxidation Products, Chem. Rev., 118, 3337-3390, https://doi.org/10.1021/acs.chemrev.7b00439, 2018.

Wolfe, G. M., Marvin, M. R., Roberts, S. J., Travis, K. R., and Liao, J.: The Framework for 0-D Atmospheric Modeling (F0AM) v3.1, Geosci. Model Dev., 9, 3309-3319, https://doi.org/10.5194/gmd-9-3309-2016, 2016.

Wormhoudt, J., Wood, E. C., Knighton, W. B., Kolb, C. E., Herndon, S. C., and Olaguer, E. P.: Vehicle emissions of radical precursors and related species observed in the 2009 SHARP campaign, J. Air Waste Manage. Assoc., 65, 699-706, https://doi.org/10.1080/10962247.2015.1008654, 2015.

Wu, C., Bell, D. M., Graham, E. L., Haslett, S., Riipinen, I., Baltensperger, U., Bertrand, A., Giannoukos, S., Schoonbaert, J., El Haddad, I., Prevot, A. S. H., Huang, W., and Mohr, C.: Photolytically induced changes in composition and volatility of biogenic secondary organic aerosol from nitrate radical oxidation during night-to-day transition, Atmos. Chem. Phys., 21, 14907-14925, 10.5194/acp-21-14907-2021, 2021.

Wu, C., Wang, C., Wang, S., Wang, W., Yuan, B., Qi, J., Wang, B., Wang, H., Wang, C., Song, W., Wang, X., Hu, W., Lou, S., Ye, C., Peng, Y., Wang, Z., Huangfu, Y., Xie, Y., Zhu, M., Zheng, J., Wang, X., Jiang, B., Zhang, Z., and Shao, M.: Measurement report: Important contributions of oxygenated compounds to emissions and chemistry of volatile organic compounds in urban air, Atmos. Chem. Phys., 20, 14769-14785, https://doi.org/10.5194/acp-20-14769-2020, 2020.

Xiao, S. and Bertram, A. K.: Reactive uptake kinetics of NO3 on multicomponent and multiphase organic mixtures containing unsaturated and saturated organics, Phys. Chem. Chem. Phys., 13, 6628-6636, https://doi.org/10.1039/C0CP02682D, 2011.

Xu, L., Suresh, S., Guo, H., Weber, R. J., and Ng, N. L.: Aerosol characterization over the southeastern United States using high-resolution aerosol mass spectrometry: spatial and seasonal variation of aerosol composition and sources with a focus on organic nitrates, Atmos. Chem. Phys., 15, 7307-7336, https://doi.org/10.5194/acp-15-7307-2015, 2015.

Xu, W., Takeuchi, M., Chen, C., Qiu, Y., Xie, C., Xu, W., Ma, N., Worsnop, D. R., Ng, N. L., and Sun, Y.: Estimation of particulate organic nitrates from thermodenuder–aerosol mass spectrometer measurements in the North China Plain, Atmos. Meas. Tech., 14, 3693-3705, https://doi.org/10.5194/amt-14-3693-2021, 2021.

Ye, C., Yuan, B., Lin, Y., Wang, Z., Hu, W., Li, T., Chen, W., Wu, C., Wang, C., Huang, S., Qi, J., Wang, B., Wang, C., Song, W., Wang, X., Zheng, E., Krechmer, J. E., Ye, P., Zhang, Z., Wang, X., Worsnop, D. R., and Shao, M.: Chemical characterization of oxygenated organic compounds in the gas phase and particle phase using iodide CIMS with FIGAERO in urban air, Atmos. Chem. Phys., 21, 8455-8478, https://doi.org/10.5194/acp-21-8455-2021, 2021.

Yu, K., Zhu, Q., Du, K., and Huang, X.-F.: Characterization of nighttime formation of particulate organic nitrates based on high-resolution aerosol mass spectrometry in an urban atmosphere in China, Atmos. Chem. Phys., 19, 5235-5249, https://doi.org/10.5194/acp-19-5235-2019, 2019.

Yuan, B., Liu, Y., Shao, M., Lu, S., and Streets, D. G.: Biomass Burning Contributions to Ambient VOCs Species at a Receptor Site in the Pearl River Delta (PRD), China, Environ. Sci. Technol., 44, 4577-4582, https://doi.org/10.1021/es1003389, 2010.

Yuan, B., Koss, A. R., Warneke, C., Coggon, M., Sekimoto, K., and de Gouw, J. A.: Proton-Transfer-Reaction Mass Spectrometry: Applications in Atmospheric Sciences, Chem. Rev., 117, 13187-13229, https://doi.org/10.1021/acs.chemrev.7b00325, 2017.

Zhang, J. K., Cheng, M. T., Ji, D. S., Liu, Z. R., Hu, B., Sun, Y., and Wang, Y. S.: Characterization of submicron particles during biomass burning and coal combustion periods in Beijing, China, Sci. Total Environ., 562, 812-821, https://doi.org/10.1016/j.scitotenv.2016.04.015, 2016.

Zhao, Y., Thornton, J. A., and Pye, H. O. T.: Quantitative constraints on autoxidation and dimer formation from direct probing of monoterpene-derived peroxy radical chemistry, Proc. Natl. Acad. Sci. U. S. A., 115, 12142-12147, https://doi.org/10.1073/pnas.1812147115, 2018.

Zhao, Y., Nguyen, N. T., Presto, A. A., Hennigan, C. J., May, A. A., and Robinson, A. L.: Intermediate Volatility Organic Compound Emissions from On-Road Gasoline Vehicles and Small Off-Road Gasoline Engines, Environ. Sci. Technol., 50, 4554-4563, https://doi.org/10.1021/acs.est.5b06247, 2016.

Zhao, Z., Husainy, S., Stoudemayer, C. T., and Smith, G. D.: Reactive uptake of NO3 radicals by unsaturated fatty acid particles, Phys. Chem. Chem. Phys., 13, 17809-17817, https://doi.org/10.1039/c1cp21790a, 2011.

Zhu, Q., He, L. Y., Huang, X. F., Cao, L. M., Gong, Z. H., Wang, C., Zhuang, X., and Hu, M.: Atmospheric aerosol compositions and sources at two national background sites in northern and southern China, Atmos. Chem. Phys., 16, 10283-10297, 10.5194/acp-16-10283-2016, 2016.